FINAL REPORT

PLASMA STABILIZATION IN LOW-POWER C BAND MICROWAVE ARCJETS

MICHAEL M. MICCI

THE PENNSYLVANIA STATE UNIVERSITY

Department of Aerospace Engineering
233 Hammond Bldg.
University Park, PA 16802

Ph: 814-863-0043
Fax: 814-865-7092
micci@psu.edu

GRANT NUMBER: F49620-97-1-0117

START DATE OF GRANT: 1 March 1997

END DATE OF GRANT: 31 October 1999

Summary

A microwave thruster with a resonant cavity sized to operate in the TM_{011} mode at 7.5 GHz and 100 Watts of power was designed and fabricated. Due to the use of C band microwave radiation the interior cavity dimensions are only 1.3 inches in diameter by 2.0 inches long, allowing a concentration of the available microwave power in the small chamber volume and providing better coupling between the microwave-heated plasma and the cold injected propellant gas. . In order to obtain thrust and specific impulse data without the effect of buoyancy forces, a vertical mechanical thrust stand designed to operate in the Penn State Propulsion Engineering Research Center vacuum facility was designed, fabricated and calibrated. A Linear Voltage Displacement Transducer (LVDT) has been integrated into the design, enabling a thrust resolution as high as 0.5 mN. Cold-gas testing of the microwave thruster with helium and nitrogen propellant using only a converging nozzle for exhausting into the laboratory ambient conditions was conducted to verify performance under unheated gas conditions.

An experimental investigation of a microwave resonant cavity thruster was conducted with the objective of characterizing the engine's performance. A 7.5 GHz engine operating with less than 100 W of input power has been tested under vacuum conditions in order to simulate the engine's behavior in realistic space conditions. Various propellants have been used, including helium (see Figure 1), nitrogen and ammonia over a wide range of specific powers. Stable plasmas could be achieved at pressure levels up to 55 psia for helium and nitrogen propellants, and up to 7 psia using ammonia propellant. Mean chamber temperatures have been measured for all three

propellants, yielding values as high as 1800 K for helium and 2100 K for nitrogen. As expected, the inlet temperature for ammonia propellant is relatively low, around 1250 K, since some of the microwave power absorbed by the ammonia gas goes into various energy storage modes such as vibrational or rotational modes instead of raising the propellant temperature.

Electron temperature measurements have been made by analyzing the spectrum of the light emitted by the 7.5 GHz thruster during atmospheric helium firings at four different wavelengths. Electron temperature values were calculated employing the relative line intensity technique, and the commonly-made assumption of Local Thermodynamic Equilibrium (LTE) was examined at various pressure levels. It has been shown that the electron temperature would converge towards a single value around 4000 K as the pressure would reach approximately 50 psia. This value is lower than those produced during previous investigations using much higher input power levels (>800 W). Doppler shift measurements of the light emitted by the exhaust plume in vacuum have been performed in order to evaluate the ejection velocity of the gas in the exit plane of a 52:1 area ratio nozzle. High spectral resolution measurements were made possible by the use of a Fabry-Perot interferometer combined with a spectrometer. Two high-transmittance fiber optic cables were used in order to simultaneously collect the light from different angular positions and carry the signal through the vacuum tank. The Doppler shift was measured using the helium emission line located at 5876 Å. Centerline specific impulses have been measured for specific powers ranging from 15 MJ/Kg up to 30 MJ/Kg (see Figure 2). Values for the centerline specific impulse as high as 1330 seconds have been recorded

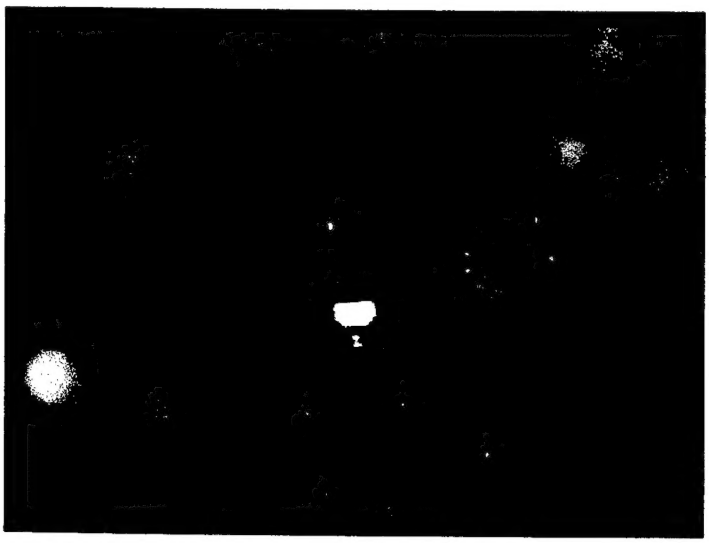

Figure 1. 7.5 GHz thruster firing on helium in vacuum chamber.

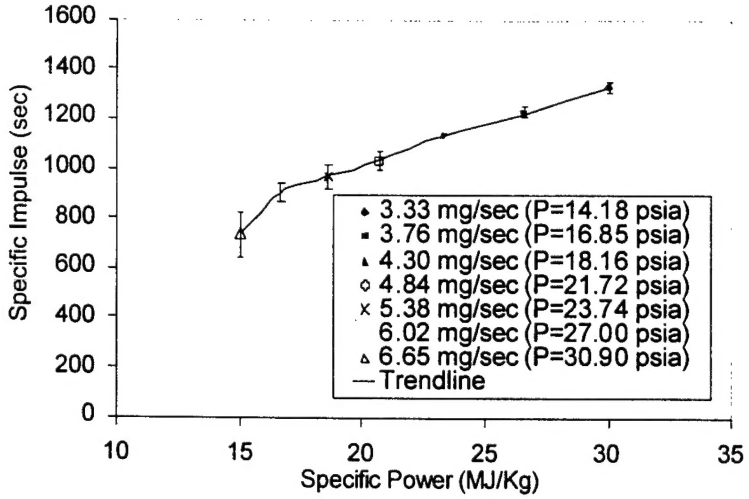

Figure 2. Centerline specific impulses vs. specific power for helium propellant.

Accomplishments/New Findings:

High specific impulses have been measured on the nozzle exit centerline using helium propellant, giving a value of 1300 seconds using only 80 Watts of input microwave power.

Personnel Supported:

Faculty: Dr. Michael M. Micci

Graduate Students: David Nordling
Frederic Souliez

Publications

"Low-Power Microwave Arcjet Testing: Plasma Plume Diagnostics and Performance Evaluation," F. J. Souliez, S. G. Chianese, G. H. Dizac and M. M. Micci. Accepted for publication in AIAA Micropropulsion Progress Series, July 2000.

Interactions:

a. "Plasma Stabilization in Low-Power C Band Microwave Arcjets", presented at the AFOSR Space Propulsion and Power Contractor Meeting, July 28-31, 1997, San Diego, CA.

"Low-Power Microwave Arcjet Performance Testing," presented at the International Electric Propulsion Conference, Aug. 25-28, 1997, Cleveland, OH.

"Rocket Propulsion Using Microwave-Heated Plasmas", presented at the University of Southern California, Department of Aerospace Engineering, Sept. 10, 1997.

"Microwave-Generated Plasmas for Combustion Enhancement", presented at the Air Force Research Laboratory, Propulsion Directorate East, Wright-Patterson AFB, OH, March 24, 1998.

"Low-Power Microwave Arcjet Testing", presented at the 34th AIAA/ASME/SAE/ASEE Joint Propulsion Conference, Cleveland, OH, July 13-15, 1998.

"Low-Power Microwave Arcjet Testing: Plasma Plume Diagnostics and Performance Evaluation," presented at the 35th AIAA/ASME/SAE/ASEE Joint Propulsion Conference, Los Angeles, CA, June 20-24, 1999.

b. One day meeting with Dr. Abdollah Nejad, Wright Laboratory, Wright-Patterson A.F.B., Dayton, Ohio, May 20, 1997, to discuss interactions between microwave-heated plasmas and supersonic combustion.

On sabbatical leave at Air Force Phillips Laboratory, Edwards A.F.B., from June 1997 to work with Dave Weaver and his research group on laser diagnostics for nozzle exit plane and plume measurements for low power microwave arcjets.

c. Transitions: One day meeting with Drs. W. Scott Best and Sandy Witman of Dupont, Inc. on August 6, 1997 to discuss use of microwave arcjet derivative for plasma material processing.

New discoveries, inventions or patent disclosures: None.

Honors/Awards: The microwave arcjet was selected as one of the top four technological inventions for 1997 in the Aviation/Aerospace category by Discover Magazine and featured in the July 1997 issue of the magazine.

Theses:

David A. Nordling, *High-Frequency Low-Power Microwave Arcjet Thruster Development*, M.S. Thesis, The Pennsylvania State University, August 1998.

Frederic J. Souliez, *Low-Power Microwave Arcjet Spectroscopic Diagnostics and Performance Evaluation*, M.S. Thesis, The Pennsylvania State University, August 1999.

AFRL-SR-BL-TR-00- 2000

0311

REPORT DOCUMENTATION PAGE

1. REPORT DATE (DD-MM-YYYY)	2. REPORT TYPE	3. DATES COVERED (From - To)
05-05-2000	Final	01 Mar 1997 - 31 Oct 1999

4. TITLE AND SUBTITLE
Plasma Stabilization in Low-Power C Band Microwave Arcjets

5a. CONTRACT NUMBER

5b. GRANT NUMBER
F49620-97-1-0117

5c. PROGRAM ELEMENT NUMBER
61102F

6. AUTHOR(S)
Micci, Michael M.

5d. PROJECT NUMBER
2308

5e. TASK NUMBER
AX

5f. WORK UNIT NUMBER

7. PERFORMING ORGANIZATION NAME(S) AND ADDRESS(ES)
The Pennsylvania State University
110 Technology Center Bldg.
University Park, PA 16802-7000

8. PERFORMING ORGANIZATION REPORT NUMBER

9. SPONSORING/MONITORING AGENCY NAME(S) AND ADDRESS(ES)
Air Force Office of Scientific Research
801 North Randolph Road
Room 732
Arlington, VA 22203-1977

10. SPONSOR/MONITOR'S ACRONYM(S)
AFOSR/NA

11. SPONSOR/MONITOR'S REPORT NUMBER(S)

12. DISTRIBUTION/AVAILABILITY STATEMENT
Approved for public release; distribution is unlimited.

13. SUPPLEMENTARY NOTES

14. ABSTRACT Performance evaluation of a 100 Watt 7.5 GHz resonant cavity microwave thruster was conducted using helium, nitrogen and ammonia propellants exhausting to both atmospheric and vacuum conditions. Emission spectroscopy of the plasma was made in order to measure the plasma electron temperature at different specific power levels, and the assumption of Local Thermodynamic Equilibrium (LTE) was examined. Electron temperature values of approximately 4000 Kelvin were measured. In order to obtain specific impulse data under vacuum conditions, the Doppler shift between light emitted by the exhaust plume parallel and perpendicular to the gas flow was measured using a high resolution Fabry-Perot interferometer. Centerline specific impulse values were obtained for helium propellant at various specific powers with a maximum value of 1330 seconds measured.

15. SUBJECT TERMS
Electric propulsion, microwave propulsion

16. SECURITY CLASSIFICATION OF:			17. LIMITATION OF ABSTRACT	18. NUMBER OF PAGES	19a. NAME OF RESPONSIBLE PERSON
a. REPORT	b. ABSTRACT	c. THIS PAGE			Dr. Mitat Birkan
U	U	U	UU	5	19b. TELEPHONE NUMBER (Include area code) 703-696-7234

AIAA 98-3499

LOW-POWER MICROWAVE ARCJET TESTING

D. Nordling, F. Souliez, M. M. Micci
Department of Aerospace Engineering and
Propulsion Engineering Research Center
The Pennsylvania State University
University Park, PA

34th AIAA/ASME/SAE/ASEE
Joint Propulsion Conference & Exhibit
July 13-15, 1998 / Cleveland, OH

LOW-POWER MICROWAVE ARCJET TESTING

D. Nordling†, F. Souliez †, M. M. Micci*
Department of Aerospace Engineering & Propulsion Engineering Research Center

The Pennsylvania State University
University Park, PA USA

Abstract

The microwave arcjet is an electrothermal propulsion device which can function at low power levels (100 Watts CW) suitable for microsatellite applications. Its electrodeless design allows it to provide steady and stable operation with negligible erosion to the device. The free-floating plasma within the resonant cavity couples the incident electrical power directly to the tangentially injected propellant gas. The plasma forms by focusing the microwave energy into the first transverse magnetic mode and operates independent of the type of propellant gas used. Two devices of this type are investigated, one operating at a frequency of 2.45 GHz and the other at 7.5 GHz. Thrust and specific impulse measurements were made with the 7.5 GHz device.

Nomenclature

a	radial dimension of the cylinder cavity (m)
h	height dimension of the cylinder cavity (m)
p	pressure (kPa)
T	temperature (Kelvins)
m	propellant mass flow rate (mg/sec)
g	gravitational acceleration at sea level (9.81 m/sec/sec)
I_{sp}	specific impulse (sec)
P	electrical power (W)
u	gas velocity (m/sec)
c	speed of light (m/sec)

Greek Symbols

χ_{01}	first zero of the Bessel function, J_0 (approximately 2.405)
μ	permeability of the media within cavity (H/m)
η	efficiency (dimensionless)
ε	permittivity of the media within cavity (F/m)
τ	Thrust force (mN)
ρ	density (kg/m^3)
ν	frequency (Hz)
λ	wavelength (m)
θ	radial coordinate (deg)

Superscripts

·	time rate of change
-	mean property

Subscripts

o	stagnation
sp	specific (per mass value)
inp	input
cav	cavity
fwd	forward
refl	reflected

Introduction

Electrothermal propulsion is a working concept in today's world. Lockheed-Martin now offers arcjets as a high-performance alternative for geosynchronous communication satellite North-South station-keeping. However, these conventional arcjets suffer from cathode erosion problems[1] as well as decreased efficiency when operating in lower (~100 W) power ranges[2]. They also cannot operate efficiently in a pulsed mode required for attitude control. Resistojets also have a material-based limitation that the propellant gas temperature can not exceed the maximum allowable temperature of the heating element or any other propellant-wetted surface.

The microwave arcjet is an electrothermal thruster concept which is electrodeless and therefore doesn't suffer life limitations of electrode erosion. A systematic illustration is given in Figure 1 showing the major components of a microwave propulsion system.

† Graduate Research Assistant, Student Member AIAA
* Professor, Associate Fellow AIAA

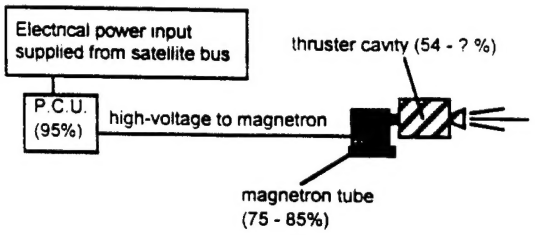

Figure 1: System illustration with component efficiencies.

Electrical power from the spacecraft electrical bus is input to a power-conditioning unit (PCU) to convert the available electrical power to high voltage. This high voltage is needed to power a microwave magnetron tube inputting its signal into a properly sized resonant thruster cavity. The cold propellant gas is fed into this engine cavity and heated by contacting the free-floating plasma discharge formed by the microwave energy exciting free electrons. This heating process thus converts the incident electrical power to thermal energy in the gas. A nozzle at the downstream end of the engine provides the final conversion of thermal energy into directed kinetic energy or thrust. This design has been tested and proven to be effective with propellants such as gaseous nitrogen, helium, hydrogen, ammonia and water vapor.

The experimental proof-of-concept studies by Balaam and Micci[3] and Mueller and Micci[4] showed the microwave propulsion concept to be viable. Mueller and Micci[4] used waveguides with internal quartz vessels to bring propellant gas in contact with the resonant transverse-magnetic fields produced within the waveguide at a frequency of 2.45 GHz and power levels of 250 W to 2 kW. Good coupling efficiency between the incident electric power and the absorption and heating of the propellant gas was demonstrated. They showed that a boron-nitride bluff-body could be used to stabilize the plasma location in the propellant flow by creating a point where the fluid velocity down the chamber would exactly balance the plasma discharge's propagation velocity toward the source of microwave energy.

Spectroscopic measurements performed by both Mueller and Micci[4] and Balaam and Micci[3] determined the electron temperature of the plasma to be about 12,000 K. This temperature was found to be relatively invariant with input power, pressure or mass-flow. Balaam and Micci[3] showed the radial profile measurements of the plasma's electron temperature to be fairly constant with input power and pressure. Due to gas pressures of one atmosphere or higher, the electron temperature was felt to be equal to the heavy particle temperature.

Balaam and Micci[3] used swirling of the propellant flow to keep the plasma located in the axial center of the circular waveguide. The axial swirling would create a region of low pressure in the center which would keep the plasma stable. A bluff-body was also used to stabilize the plasma location within the cavity. This method of stabilization was demonstrated with helium plasmas up to 500 kPa gas pressures and coupling efficiencies between 95 - 100% were obtained. Nitrogen also showed similarly good coupling efficiency but was found to be more difficult to ignite due to a greater number of internal energy modes of the diatomic molecules. Although the swirling method did not prove to be as successful as the bluff body, the quality of the swirling motion was probably affected by the geometry of the quartz vessel used.

Sullivan[5] demonstrated a reliable design to produce plasmas in a resonant cylindrical cavity using swirl-injection of the propellant. Sullivan's design, operating in the TM_{011} mode, which better concentrated the electric field along the axis of the chamber, also included the use of a dielectric separation plate to isolate the plasma region from contacting the antenna portion of the engine. Axisymmetric power coupling from the microwave generation source to the microwave arcjet resonant cavity was achieved by aligning a linear probe into the cavity along the longitudinal axis of symmetry of the cylindrical cavity. The linear probe or antenna was simply the termination of the coaxial power transmission line as it entered the cavity. By adjusting the probe's depth into the cavity and adjusting the overall length of the cylindrical cavity, the load impedance of the cavity and the impedance of the transmission line could be matched. When the two system impedances are matched, the maximum amount of power will be absorbed by the cavity/plasma system.

Kline[6] performed actual vacuum chamber thrust stand measurements. Unlike Sullivan's thruster, Kline's magnetron was rigidly mounted into the body of the thruster. This work provided the first vacuum chamber thrust measurements of a microwave arcjet at a frequency of 2.45 GHz and showed a thruster efficiency of 54% (thrust power divided by input electrical power). Kline operated in the 600 to 800 W incident power range and demonstrated a maximum thrust of 303 mN.

The work discussed here uses frequencies of 7.5 GHz and 2.45 GHz at lower input power levels (~100 W). The 7.5 GHz and 2.45 GHz magnetrons, manufactured by Mictron, are voltage-tunable which allows the frequency of the microwave signal to be fine-tuned by adjusting the supplied voltage to optimize power coupling into the cavities while maintaining a fixed thruster geometry. The results of

Kline showed the efficiency of a microwave arcjet engine to be relatively constant with input electrical power.

The best propellants for this system have been shown to be low molecular-weight, monatomic gases.[5] But for practical purposes, a liquid-storable propellant would be preferred for easy, on-orbit storage. Helium and hydrogen are both difficult to store for extended periods of time due to their extremely low boiling points. Ammonia (NH_3) has been selected for its higher-temperature, liquid-storable properties and low molecular weight. Water (H_2O) is also a good propellant in these respects.

Magnetron efficiency at a frequency of 7.5 GHz can be increased to as much as 75% with possible improvements to the magnetron design by the manufacturer, Mictron, Inc.[7]. The efficiency increases with decreasing frequency, becoming 85% at a frequency of 2.45 GHz. It is believed that through greater optimization of the engine cavity and nozzle and lowered frozen flow losses from the propellant, a greater thruster efficiency can be attained.

Experiment

The system introduces the microwave signal into a cylindrical, conductive closed cavity where the first transverse-magnetic mode (TM_{011}) is resonant within the cavity. The cylindrical cavity is sized by Equation 1 from Balanis[8]. μ and ε are the permeability and permittivity constants, where the inverse square root of the product of these two factors represent the phase velocity of the electromagnetic wave.

$$(f_r)_{01p}^{TM} = \left(\frac{1}{2\pi\sqrt{\mu\varepsilon}}\right)\sqrt{\left(\frac{\chi_{01}}{a}\right)^2 + \left(\frac{p\pi}{h}\right)^2} \qquad (1)$$

The engine is illustrated in Figure 2. The cavity is partitioned in two halves separated by a dielectric, quartz plate. The propellant is swirl-injected tangentially in the nozzle side of the cavity (plasma chamber). This is done for both cooling of the chamber interior walls and for axial stability of the plasma. The other side near the antenna (upper chamber) is kept pressurized to ensure that the plasma formation takes place only in the plasma chamber where the propellant is fed in at lower pressure and brought slowly up to the desired chamber pressure. The engine's plasma chamber has two sets of injection holes, one pair near the separation plate and the other pair near the nozzle, to determine the effect of swirl port location on the stability of the plasma near the nozzle. The plasma is created by the region of high electromagnetic field strength formed at the center of the cavity near the nozzle. The propellant gas is heated by being forced to flow in close contact to the plasma as it expands through the nozzle converting thermal energy to directed kinetic energy, creating thrust.

An observation window is on the side of the thruster for viewing into the plasma chamber to verify plasma stability and location. The holes in the metal body for this viewing window (as well as the 0.25mm nozzle throat) are too small to allow a significant portion (less than 0.1% of incident power) of the microwave energy to exit the cavity. The body of engine is aluminum while the nozzle plate is stainless steel for greater survivability in the event that the plasma should briefly contact the nozzle plate.

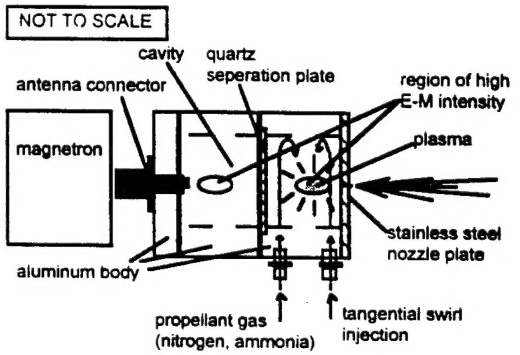

Figure 2: Engine Schematic.

Test Facility

The experimental setup, shown in Figure 3, consisted of a propellant gas bottle supply attached to UNIT Instruments, UTS-8100, 750 sccm NH_3, digital mass-flow controller. Other UNIT mass flow controllers were available for testing. (30 SLM, N_2 and 5 SLM, N_2) The propellant lines feed into a vacuum facility which is capable of slightly less than 1 torr of pressure during operation of the thruster while operating with the Stokes mechanical pump only. The power-supply is outside of the vacuum chamber.

The engine testing assembly consists of the magnetron, coupler, and engine cavity. The magnetron is the microwave generating device that feeds through a dual-directional coupler for forward and reflected power measurements. The coupler is not essential to the function of the device, only the magnetron and engine cavity (plus any hard

waveguide or coaxial connection between the two). The coupler is present for testing purposes and gives negligible effect on performance. The coupler then attaches to the engine's antenna connector and the engine cavity serves as the load.

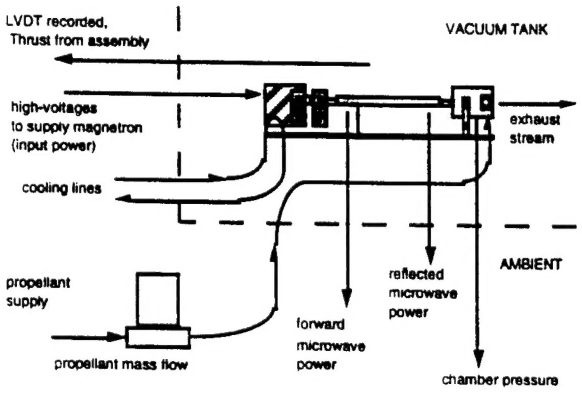

Figure 3: Experimental setup.

An (inverted pendulum design was used for the thrust stands. The thruster assembly sits on top of thin shims that deflect and flex sideways under small thrust loads. The general design is illustrated in Figures 4a and 4b below.

Fig. 4a: Photo of inverted thrust stand

The initial goals of this program are to experimentally obtain values for thrust, specific impulse and thruster efficiency at low microwave power levels. Each of these values are obtained from

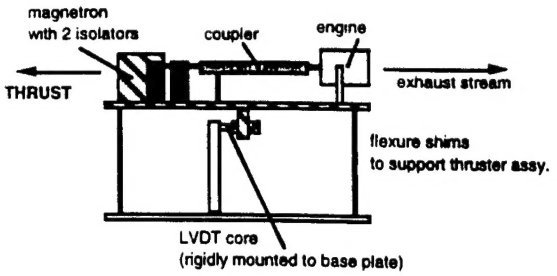

Fig. 4b: Inverted pendulum thrust stand

mass flow and thrust measurements. Equations 2 through 4 show the formulas for computing specific impulse, specific power and overall thermodynamic efficiency, respectively. Mass flow measurements come from the UNIT mass flow controller with calibration traceable to NIST standards. The engine cavity efficiency can also be determined by the forward and reflected power readings of the dual-directional coupler. Magnetron efficiency can be estimated by comparing the forward power meter reading against the input power drawn into the magnetron from the supply. This magnetron efficiency also incorporates the losses from the connectors between the magnetron, isolators, and coupler. Equations 5 and 6 show the computing formulas for these values.

$$I_{sp} = \frac{\tau}{mg} \quad (2)$$

$$P_{sp} = \frac{P_{fwd} - P_{refl}}{m} \quad (3)$$

$$\eta_{overall} = \frac{\tau^2}{2 \cdot m \cdot P_{input}} \quad (4)$$

$$\eta_{cav} = \frac{P_{fwd} - P_{refl}}{P_{fwd}} \quad (5)$$

$$\eta_{magnetron} = \frac{P_{fwd}}{P_{input}} \quad (6)$$

Known weights are suspended from a single human hair attached to the thruster assembly and draped perpendicularly over a piece of PFA tubing to accurately calibrate the pendulum thrust stand. This calibration is done with up to ten different weights ranging from 0.265 to 1.12 grams, which translates to forces ranging from 2.6 to 11.0 mN. The calibration is always done prior to each series of tests to check

and update the accuracy and response of the thrust stand. Figure 5 shows typical calibration curves prior to cold-gas testing. The curves are generated at least once per day of testing to compensate for variation.

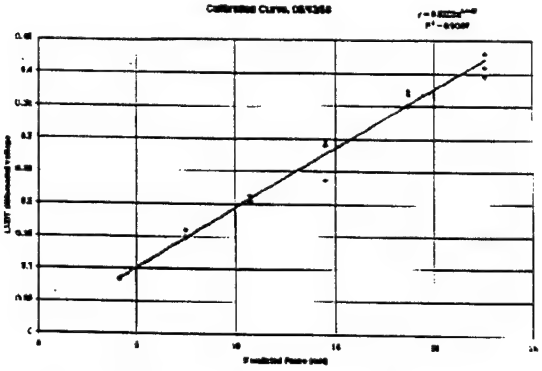

Figure 5: Inverted thrust stand calibration.

7.5 GHz Thruster Experimentation

Hot firing of the 7.5 GHz thruster with helium gas has been demonstrated. A photo of a thruster firing is shown in Figure 6.

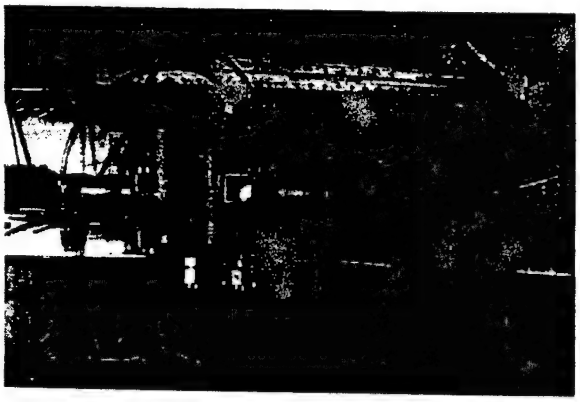

Figure 6: Photo of 7.5 GHz hot-firing.

Testing so far on the 7.5 GHz prototype has been done in ambient conditions. A Welch vacuum pump fitted with a small suction cup to cover the engine s nozzle was used to simulate the necessary vacuum start conditions. This setup was also used in the testing of the 2.45 GHz prototype to be mentioned in the next section.

The thruster was vacuum started at a chamber pressure of 4-5 torr. The plasma formed reliably and instantly at this pressure once the microwave power was switched on. The propellant flow was immediately increased and the chamber pressure was brought to slightly above ambient pressure. The suction cup was removed and engine continued stable operation. Propellant flow was brought to 100% (4.428 mg/sec, helium gas) of the mass-flow controller s capacity with a stable plasma in place. Cold flow data was obtained for both helium and nitrogen. Tabulated vacuum-start hot-fire results in Table 1.

mass flow (mg/sec)	3.54	4.43	1.77
chamber pressure (kPa, absolute)	138	155	105
Forward Power (W)	102	85	86
Reflected Power (W)	9	< 1	< 1
Specific Power (MJ/kg)	26.27	19.19	48.59

Table 1. Helium Vacuum-start Data, 7.5 GHz

Ambient thrust measurements were made with the 7.5 GHz thruster using a wire-start method for ambient pressure ignition. Using a tungsten wire, the plasma can be started only in the plasma chamber at atmospheric pressure. Testing demonstrated helium plasmas at power levels of almost 100 Watts. Mass flow, chamber pressure, forward and reflected microwave power measurements were made. Hot-fire testing was done in ambient laboratory conditions with a converging nozzle. This nozzle was necessary due to the design constraint of 2 atmospheres maximum differential pressure allowed across the separation plate. Vacuum testing will allow higher area-ratio nozzles (up to 52:1) to be effective. Results of hot-fire testing of helium and nitrogen propellants are given in Tables 2a, 2b, and 2c.

Input power from the supply was around 160 Watts for the 7.5 GHz magnetron. The measured forward power was 80 to 100 Watts. Reflected power at vacuum startup was at most 40 Watts, but the amount of reflected power dropped to negligible levels (less than 1 Watt) once the chamber pressure was above 1/2 atmosphere (absolute). Vacuum starts with nitrogen has been unsuccesful so far. Testing continues to achieve firings with nitrogen and other polyatomic propellants.

2.45 GHz Thruster Experimentation

As stated earlier, a similar 7.5 GHz thruster is currently being tested at the same time as the 2.45 GHz engine. Both have practical and theoretical advantages. The concept of free-floating plasma has already been explained in a previous paper[11].

mass flow (mg/sec)	4.43	4.43	4.43	3.54	3.54	2.66	2.66
cold flow thrust (mN)	2.29	2.09	1.95	–	–	–	–
cold specific impulse (sec)	52.63	48.12	44.94	–	–	–	–
ideal specific impulse (sec)	58.59	58.59	58.59	–	–	–	–
specific power (MJ/kg)	20.10	17.31	17.83	25.16	25.16	34.82	34.38
hot-fire thrust (mN)	5.57	6.16	7.66	4.12	4.02	1.37	2.65
hot-fire specific impulse (sec)	128.3	141.8	176.3	118.5	115.6	52.4	101.7

Table 2a. Thrust Stand Measurements for Helium Propellant with Converging Nozzle.

mass flow (mg/sec)	21.444	21.444	21.444
cold flow thrust (mN)	6.53	6.16	5.98
specific impulse (seconds)	31.04	29.30	28.43
ideal specific impulse (seconds)	32.14	32.01	32.01

Table 2b. Thrust Stand Measurements for Nitrogen Cold Flow, Converging Nozzle.

mass flow (mg/sec)	6.43	10.72	10.72	10.72	15.01	15.01	19.30
specific power (MJ/kg)	17.23	9.70	9.70	9.38	6.70	6.85	5.39
hot-fire thrust (mN)	4.47	13.77	5.92	5.98	8.91	9.28	9.00
hot-fire specific impulse (seconds)	70.9	130.9	56.3	56.9	60.5	63.0	47.6

Table 2c. Thrust Stand Measurements for Nitrogen Propellant with Converging Nozzle.

However it is of interest to underline a few differences in the plasma behavior between the two operating frequencies. In both cases the breakdown occurs when the electromagnetic field frequency is high enough that the direction of the force on the charged particles is changed before they can travel too far and leave the discharge area. A more compact plasma is therefore obtained at higher frequencies. Moreover, the cavity is sized by Equation 1 and its length can be reduced at higher frequencies. Hence the 7.5 GHz thruster will be lighter and convective heat losses from the plasma to the cavity will also be lower since the total chamber-wall heat transfer rate decreases as size is decreased[9]. This should help to stabilize the plasma since it reduces the plasma's tendency to expend more energy than it absorbs from the field which leads to its spontaneous extinction. The shorter cavity length is therefore likely to yield a higher thrust-to-weight ratio.

However, the current work being done at Penn State University on the 2.45 GHz shows that this operating frequency is still of interest for the projected applications of the microwave arcjet. As mentioned earlier, the magnetron efficiency increases with decreasing frequency. At 2.45 GHz it is assumed to be on the order of 85%, whereas magnetron efficiency at a frequency of 7.5 GHz can only be increased to 75% with improvements to its design by the manufacturer. It is also experimentally demonstrated that the breakdown of gases due to microwaves is likely to take place at lower E/ρ ratios at a lower resonant frequency[10]. Breakdown fields for different frequencies are shown in Figure 9. This means that the 2.45 GHz thruster efficiency is expected to be higher than that of the 7.5 GHz thruster. Equation 3 shows that if the same amount of thrust can be generated with a lower electrical power input then we achieve a higher overall thermodynamic efficiency. The presence of the separation plate has a minor effect on the overall resonant field pattern within the cavity. However the impact of this quartz plate on the field could be more important in the 7.5 GHz thruster where the relative size of the plate compared to the size of the cavity is larger.

The previous work done with the 2.45 GHz microwave arcjet was conducted at both high pressure (up to 800 KPa) and at high power (up to 2200 W) levels using helium, nitrogen, ammonia and hydrogen. The design of the original engine has been slightly modified to allow the use of a tunable 2.45 GHz magnetron operating in much lower (~100 W) power ranges. Some injection features have also been reconsidered in order to use smaller mass flow rates with an increased injection velocity. The major components of the system are the same as those shown in Figure 1.

The current work focuses on forming and stabilizing a plasma with helium, nitrogen, water vapor and ammonia in vacuum conditions. Some hot fire tests have already been realized with helium and nitrogen. It was possible to ignite and stabilize either a helium or a nitrogen plasma several times in a row. Reliable vacuum starts with an input power into the cavity on the order of 90 W were obtained. A vacuum pump was used to reduce the pressure in the cavity to 10 Torr in the case of helium and 1 Torr in the case of nitrogen. The tests with ammonia and water have not been completed yet due to experimental facility limitations. The plasma glows for helium and nitrogen during the vacuum start are as shown in Figure 7 and 8.

Figure 7: Plasma ignition in vacuum conditions using helium at 2 Torr.

During these vacuum starts, it has been observed that the plasma initially extended along the cavity axis. A slow increase in the mass flow rate would cause the plasma to contract to a more compact plasma located next to the nozzle inlet. This small plasma absorbs all the incident power and being located within the nozzle constitutes the optimum operating mode.

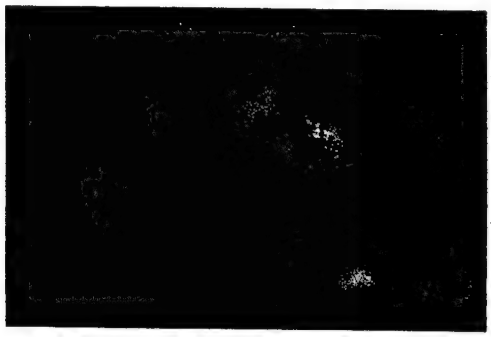

Figure 8: Plasma ignition in vacuum conditions using nitrogen at 1 Torr.

mass flow (mg/sec)	1.77	3.54	4.43
chamber pressure (kPa, absolute)	38	73	97
Forward Power (W)	81	81	80
Reflected Power (W)	20	3	< 1
Specific Power (MJ/kg)	34.46	22.03	18.05

Table 3. Helium Vacuum-start Data, 2.45 GHz

As expected a decreasing reflected power was measured with an increasing mass flow rate. A

reflected power close to zero could be achieved once the mass flow rate was above a given threshold. Testing with helium has shown to be much easier than testing with nitrogen. This is due to the monoatomic nature of helium[11] since no input energy is lost into dissociation. Another aspect is that at high temperatures the specific heat C_p increases with temperature because of energy going into vibrational modes[12]. Representative performance numbers for the helium operation are presented in Table 3. It has not been possible yet to get a cavity stagnation pressure higher than 100 kPa due to experimental facility limitations.

The use of a new mid-range mass flow controller should dramatically increase the maximum attainable pressure inside the plasma chamber. During these tests the specific power ranged from 18 MJ/Kg to 35 MJ/Kg.

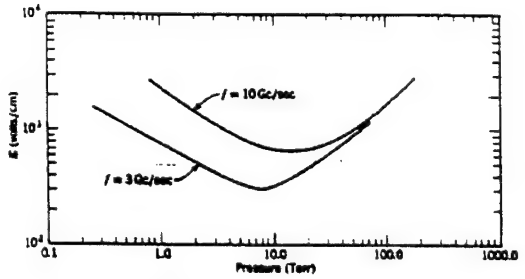

Figure 9: Breakdown fields as a function of pressure for different frequencies in a mixture of He and Hg (MacDonald, A.D., Microwave Breakdown in Gases, John Wiley & Sons, 1966)

Future Work

The future work on the 7.5 GHz and 2.45 GHz engines will be directed at determining the velocity profiles for operation with ammonia and water. It is planned to use an optical diagnostic based on Doppler shifted light. If light is emitted from a molecule moving toward a detector, the frequency of that light will be Doppler shifted. If this shift can be measured, then the velocity as which the molecule was moving toward the detector can be calculated as

$$u = c\frac{\Delta\upsilon}{\upsilon} \qquad (7)$$

This application will be emission based assuming that the gas which is going to be measured will be self-radiant. This technique as applied to electrothermal thrusters has primarily concentrated on resolving the velocity profile of the atomic hydrogen species within the exhaust plume. The advantage of this technique combined with the use of ammonia or water is that there is no need to seed the flow with hydrogen.

Previous tests have not been able to resolve the expected velocity data due to the excessive pressure broadening of the spectral lines of interest[5]. The work being conducted now concentrates on resolving the velocity profile of the plasma jet exiting the nozzle in the vacuum tank. The expected results should not be affected by pressure broadening effects in vacuum conditions.

The experimental setup consists of a pair of focusing lenses that will collect the shifted and unshifted signals at different radial locations. The Doppler shift $\Delta\nu$ is determined by comparing the shifted signal to an unshifted reference signal. The unshifted signal is determined by collecting a signal orthogonal to the plasma jet. The radial velocity should ideally be zero. Having determined two Doppler shifts $\Delta\nu_1$ and $\Delta\nu_2$ at two different radial locations (θ_1 and θ_2 respectively), the velocity components are then given by Equations 8 and 9.

$$u_x = \frac{\lambda\left[\Delta\upsilon_2 \sin\theta_1 + \Delta\upsilon_1 \sin\theta_2\right]}{\sin(\theta_1 + \theta_2)} \qquad (8)$$

$$u_y = \frac{\lambda\left[\Delta\upsilon_1 \sin\theta_2 - \Delta\upsilon 2 \sin\theta_1\right]}{\sin(\theta_1 + \theta_2)} \qquad (9)$$

The emission line will be looked for in the region between 650 nm to 660 nm since most of the work done in the field of exhaust plume characterization have used the first transition of the Balmer series of the H-atom at 656.28 nm with a corresponding frequency of 4.57×10^{14} Hz. Since the exhaust jet will be issuing from a choked nozzle, a good first-order estimate of the gas velocity is the speed of sound. For the Balmer-α transition, the estimated shift at the speed of sound is 1.89 GHz. This velocity profile can be accurately resolved provided that the measured species is one of the major species in the exhaust plume.

Conclusion

The microwave arcjet has advantages over conventional arcjets in use today. The electrodeless design eliminates cathode erosion problems associated with DC arcjet types. Due to the tangential swirl injection of the propellant for plasma stabilization, the limited chamber temperature associated with material aspects of resistojets is also increased due to the plasma's axial location and the

cold propellant gas's injection from the wall. The 12,000 K plasma formed by the resonant microwave energy should offer high specific impulse at low incident power (~ 100 W). Thrust levels of 30 mN and specific impulse values near 500 seconds are expected for water and ammonia propellants. The microwave arcjet shows great promise for low thrust applications on microsatellites.

The 7.5 GHz thruster has proved viable. Cold flow testing was performed in ambient conditions with helium and nitrogen. A helium plasma can be ignited with 20 Watts of microwave power at 5 kPa (gauge) chamber pressure. Vacuum starts of helium and nitrogen gas were done with the nominal 100 Watts of incident power (CW).

Testing with 2.45 GHz has also been successful. Helium and nitrogen firings have been demonstrated.

Future work for this project includes thrust stand measurements in vacuum. The work will include thrust, specific impulse, and thruster efficiency measurements for ammonia, nitrogen, helium, hydrogen and water vapor propellants exhausting into a vacuum. The results of the optical diagnostic will provide an exhaust velocity profile which will give both thrust measurements and a baseline to compare this device against other electric propulsion devices.

Acknowledgments

This work was supported by AFOSR Grant F49620-97-1-0117. The authors would like to thank the assistance of John Kline of Research Support Instruments, Lanham, MD.

References

1. Nordling, D. and Micci, M. M.; "Low Power Microwave Arcjet Development," IEPC 97-089, 25th International Electric Propulsion Conference, August 24-28, 1997.

2. Sankovic, J. and Hopkins, J., "Miniaturized Arcjet Performance Improvement", AIAA 96-2962, 32nd AIAA/ASME/SAE/ASEE Joint Propulsion Conference, Lake Buena Vista, FL, July 1-3, 1996.

3. Balaam, P. and Micci, M. M., "Investigation of Stabilized Resonant Cavity Microwave Plasmas for Propulsion", AIAA Journal of Propulsion and Power, Vol. 11, No. 5, September-October 1995, p. 1021 - 1027.

4. Mueller, J. and Micci, M. M., "Microwave Waveguide Helium Plasmas for Electrothermal Propulsion", AIAA Journal of Propulsion and Power, Vol. 8, No. 5, September-October 1992, p. 1017 - 1022.

5. Sullivan, D. J., "Development and Performance Characterization of a Microwave Electrothermal Thruster Prototype". Ph.D. Dissertation, Aerospace Engineering Department, Pennsylvania State University, January 1996.

6. Kline, J., "Thrust Measurements of a Microwave Electrothermal Thruster"., Master of Science Thesis, Aerospace Engineering Department, Pennsylvania State University, August 1996.

7. Weinstein, M. Mictron Inc., Sarasota, FL, *Personal Communication*, 7/7/97

8. Balanis, C. A., "Advanced Engineering Electromagnetics", 1989.

9. Hill, P.G. and Peterson, C.R., Mechanics and Thermodynamics of Propulsion, Addison-Wesley, 1992.

10. MacDonald, A.D., Microwave Breakdown in Gases, John Wiley & Sons, 1966.

11. Sullivan, D. J., M. M. Micci, "Performance Testing and Exhaust Plume Characterization of the Microwave Arcjet Thruster", AIAA 94-3127, 30th AIAA/ASME/SAE/ASEE Joint Propulsion Conference, Indianapolis, IN, June 27-29, 1994.

12. Liepmann, H.W. and Roshko, A., Elements of Gasdynamics, John Wiley & Sons, 1957.

25th

IEPC 97-089

LOW-POWER MICROWAVE ARCJET PERFORMANCE TESTING

D. Nordling and M. M. Micci
Pennsylvania State University
University Park, Pennsylvania

25th International Electric Propulsion Conference
August 24-28, 1997, Cleveland, Ohio

LOW-POWER MICROWAVE ARCJET PERFORMANCE TESTING

D. Nordling* and M. M. Micci†
Department of Aerospace Engineering and Propulsion Engineering Research Center
The Pennsylvania State University
University Park, PA, USA

Abstract

A microwave arcjet is an electrodeless electrothermal thruster. This design does not suffer from cathode erosion problems of DC arcjets or the chamber temperature limitation associated with resistojets. The system is a closed cylindrical cavity with an antenna connector at one end. The cavity is dimensioned to resonate the first transverse magnetic mode of the microwave signal (TM_{011}). Propellant is tangentially injected and contacts the plasma formed along the longitudinal axis in the nozzle-side of the chamber (opposite to the antenna) as it is exhausted through the nozzle. Prior research has demonstrated good coupling between the incident microwave energy and the propellant gas. The current design uses 7.5 GHz microwave energy at 100 W. Cold flow testing has been performed in ambient conditions with helium and nitrogen. Helium plasma was formed at a chamber pressure of 5 kPa (gauge) with 20 Watts of microwave power. Further testing will use ammonia, nitrogen, helium, hydrogen and water vapor as propellants exhausting into a vacuum.

Nomenclature

a	radial dimension of the cylinder cavity (m)
h	height dimension of the cylinder cavity (m)
p	vertical resonant mode of cavity (equal to 1)
χ_{01}	first zero of the Bessel function, J_0 (equal to approximately 2.405)
μ	permeability of the media within cavity (H/m)
ε	permittivity of the media within cavity (F/m)
τ	Thrust force (N)
m	propellant mass flow rate (kg/sec)
g	gravitational acceleration at sea level (9.81 m/sec/sec)
I_{sp}	specific impulse (sec)
P_{input}	input electrical power from supply (W)

Introduction

Electrothermal propulsion is a working concept in today's world. Lockheed-Martin now offers arcjets as a high-performance alternative for geosynchronous communication satellite North-South station-keeping. However, these conventional arcjets suffer from cathode erosion problems[1] as well as decreased efficiency when operating in lower (~100 W) power ranges[2]. Resistojets also have a material-based limitation that the propellant gas temperature can not exceed the maximum allowable temperature of the heating element or any other propellant-wetted surface.

The microwave arcjet is an electrothermal thruster concept which is electrodeless and therefore doesn't suffer life limitations of electrode erosion. A systematic illustration is given in Figure 1 showing the major components of a microwave propulsion system.

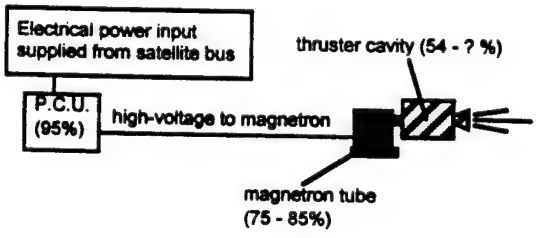

Fig. 1: System illustration with component efficiencies.

*Graduate research assistant.
†Associate Professor.

Electrical power from the spacecraft electrical bus is input to a power-conditioning unit (PCU) to convert the available electrical power to high voltage. This high voltage is needed to power a microwave magnetron tube inputting its signal into a properly sized resonant thruster cavity. The cold propellant gas is fed into this engine cavity and heated by contacting the free-floating plasma discharge formed by the microwave energy exciting free electrons. This heating process thus converts the incident electrical power to thermal energy in the gas. A nozzle at the downstream end of the engine provides the final conversion of thermal energy into directed kinetic energy or thrust. This design has been tested and proven to be effective with propellants such as gaseous nitrogen, helium, hydrogen, ammonia and water vapor.

The experimental proof-of-concept studies by Balaam and Micci[3] and Mueller and Micci[4] showed the microwave propulsion concept to be viable. Mueller and Micci[4] used waveguides with internal quartz vessels to bring propellant gas in contact with the resonant transverse-magnetic fields produced within the waveguide at a frequency of 2.45 GHz and power levels of 250 W to 2 kW. Good coupling efficiency between the incident electric power and the absorption and heating of the propellant gas was demonstrated. They showed that a boron-nitride bluff-body could be used to stabilize the plasma location in the propellant flow by creating a point where the fluid velocity down the chamber would exactly balance the plasma discharge's propagation velocity toward the source of microwave energy.

Spectroscopic measurements performed by both Mueller and Micci[4] and Balaam and Micci[3] determined the electron temperature of the plasma to be about 12,000 K. This temperature was found to be relatively invariant with input power, pressure or mass-flow. Balaam and Micci[3] showed the radial profile measurements of the plasma's electron temperature to be fairly constant with input power and pressure. Due to gas pressures of one atmosphere or higher, the electron temperature was felt to be equal to the heavy particle temperature.

Balaam and Micci[3] used swirling of the propellant flow to keep the plasma located in the axial center of the circular waveguide. The axial swirling would create a region of low pressure in the center which would keep the plasma stable. A bluff-body was also used to stabilize the plasma location within the cavity. This method of stabilization was demonstrated with helium plasmas up to 500 kPa gas pressures and coupling efficiencies between 95 - 100% were obtained. Nitrogen also showed similarly good coupling efficiency but was found to be more difficult to ignite due to a greater number of internal energy modes of the diatomic molecules. Although the swirling method did not prove to be as successful as the bluff body, the quality of the swirling motion was probably affected by the geometry of the quartz vessel used.

Sullivan[5] demonstrated a reliable design to produce plasmas in a resonant cylindrical cavity using swirl-injection of the propellant. Sullivan's design, operating in the TM_{011} mode, which better concentrated the electric field along the axis of the chamber, also included the use of a dielectric separation plate to isolate the plasma region from contacting the antenna portion of the engine. Axisymmetric power coupling from the microwave generation source to the microwave arcjet resonant cavity was achieved by aligning a linear probe into the cavity along the longitudinal axis of symmetry of the cylindrical cavity. The linear probe or antenna was simply the termination of the coaxial power transmission line as it entered the cavity. By adjusting the probe's depth into the cavity and adjusting the overall length of the cylindrical cavity, the load impedance of the cavity and the impedance of the transmission line could be matched. When the two system impedances are matched, the maximum amount of power will be absorbed by the cavity/plasma system.

Kline[6] performed actual vacuum chamber thrust stand measurements. Unlike Sullivan's thruster, Kline's magnetron was rigidly mounted into the body of the thruster. This work provided the first vacuum chamber thrust measurements of a microwave arcjet at a frequency of 2.45 GHz and showed a thruster efficiency of 54% (thrust power divided by input electrical power). Kline operated in the 600 to 800 W incident power range and demonstrated a maximum thrust of 303 mN. The work discussed here uses a frequency of 7.5 GHz to provide a smaller resonant cavity to reduce heat losses and provide a more concentrated electric field at lower input power levels (~100 W). The 7.5 GHz magnetron, manufactured by Mictron, is voltage-tunable which allows the frequency of the microwave signal to be fine-tuned by adjusting the supplied voltage to optimize

power coupling into the cavity while maintaining a fixed thruster geometry.

The results of Kline showed the efficiency of a microwave arcjet engine to be relatively constant with input electrical power. Figure 2, given below, compares the performance of Hall thrusters[7,8], a conventional arcjet[2] and pulsed arcjets[9] in terms of overall system efficiency versus input electrical along with the projected efficiency trend of a microwave arcjet system with decreasing power. It should be noted that the magnetron/microwave system is a total efficiency figure that includes the losses of all the major components of the microwave propulsion system.

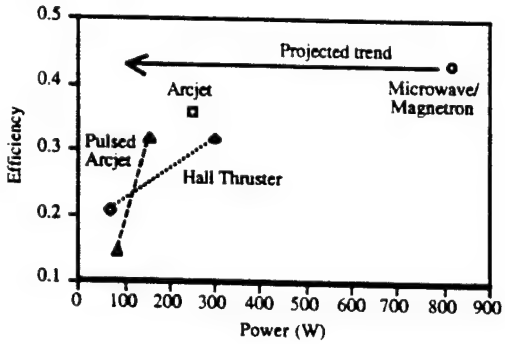

Fig. 2: Comparison chart of electric propulsion system efficiency versus input power level.

The best propellants for this system have been shown to be low molecular-weight, monatomic gases.[5] But for practical purposes, a liquid-storable propellant would be preferred for easy, on-orbit storage. Helium and hydrogen are both difficult to store for extended periods of time due to their extremely low boiling points. Ammonia (NH_3) has been selected for its higher-temperature, liquid-storable properties and low molecular weight. Water (H_2O) is also a good propellant in these respects.

The high-voltage PCU mentioned above is an existing and developed piece of hardware for powering traveling wave tubes (TWT's) used in all communications satellites. These PCU's currently operate at 95% electrical efficiency. Magnetron efficiency at a frequency of 7.5 GHz could be increased to as much as 75% with possible improvements to the magnetron design by the manufacturer, Mictron, Inc.[10]. The efficiency increases with decreasing frequency, becoming 85% at a frequency of 2.45 GHz. It is believed that through greater optimization of the engine cavity and nozzle and lowered frozen flow losses from the propellant, a greater thruster efficiency can be attained.

Experiment

The system introduces the microwave signal into a cylindrical, conductive closed cavity where the first transverse-magnetic mode (TM_{011}) is resonant within the cavity. The cylindrical cavity is sized by Equation 1 from Balanis[11]. μ and ε are the permeability and permittivity constants, where the inverse square root of the product of these two factors represent the phase velocity of the electromagnetic wave.

$$(f_r)_{01p}^{TM} = \left(\frac{1}{2\pi\sqrt{\mu\varepsilon}}\right)\sqrt{\left(\frac{\chi_{01}}{a}\right)^2 + \left(\frac{p\pi}{h}\right)^2} \qquad (1)$$

The engine is illustrated in Figure 3. The cavity is partitioned in two halves separated by a dielectric, quartz plate. The propellant is swirl-injected tangentially in the nozzle side of the cavity (plasma chamber). This is done for both cooling of the chamber interior walls and for axial stability of the plasma. The other side near the antenna (upper chamber) is kept pressurized to ensure that the plasma formation takes place only in the plasma chamber where the propellant is fed in at lower pressure and brought slowly up to the desired chamber pressure. The engine's plasma chamber has two sets of injection holes, one pair near the separation plate and the other pair near the nozzle, to determine the effect of swirl port location on the stability of the plasma near the nozzle. The plasma is created by the region of high electromagnetic field strength formed at the center of the cavity near the nozzle. The propellant gas is heated by being forced to flow in close contact to the plasma as it expands through the nozzle converting thermal energy to directed kinetic energy, creating thrust.

An observation window is on the side of the thruster for viewing into the plasma chamber to verify plasma stability and location. The holes in the metal body for this viewing window (as well as the 0.25mm nozzle throat) are too small to allow a significant portion (less than 0.1% of incident power) of the microwave energy to exit the cavity. The body of engine is aluminum while the nozzle plate is stainless steel for greater

survivability in the event that the plasma should briefly contact the nozzle plate. The test article is shown in Figure 4 below.

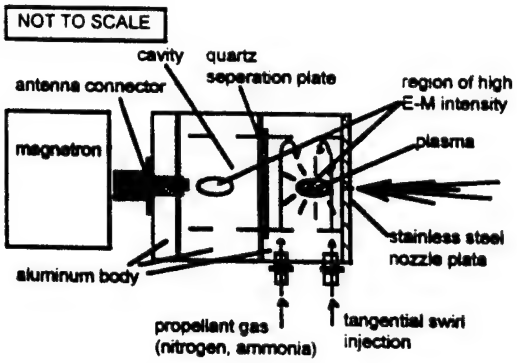

Fig. 3: Engine Schematic.

Fig. 4: Photo of Engine Test Article.

Test Facility

The experimental setup, shown in Figure 5, consisted of a propellant gas bottle supply attached to UNIT Instruments, UTS-8100, 750 sccm, digital mass-flow controller. The propellant lines feed into a vacuum facility which is capable of slightly less than 1 torr of pressure during operation of the thruster while operating with the Stokes mechanical pump only. The power-supply and microwave magnetron are also outside of the vacuum chamber. A secondary isolator is attached to the magnetron for greater safety against reflected power into the magnetron. A flexible microwave coaxial transmission cable is fed into the vacuum tank to attach to the engine's antenna connector.

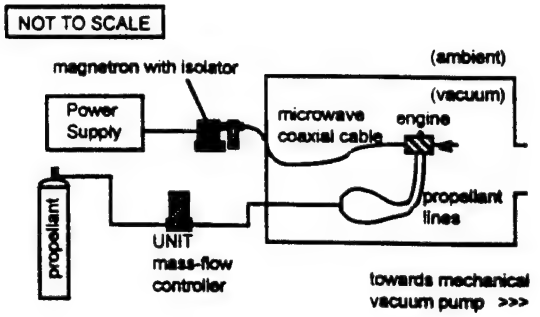

Fig. 5: Experimental setup.

A pendulum-based thrust stand was constructed to measure milliNewton range thrust levels. This thrust stand setup is illustrated in Figure 6. The engine is suspended from two pieces of 0.001" thick, stainless-steel shim stock. A displacement transducer measures the horizontal displacement of the system in inches as the thruster pushes against the gravitational restoration force in the pendulum. A force of 10 mN results in a typical displacement of 0.00485 inches.

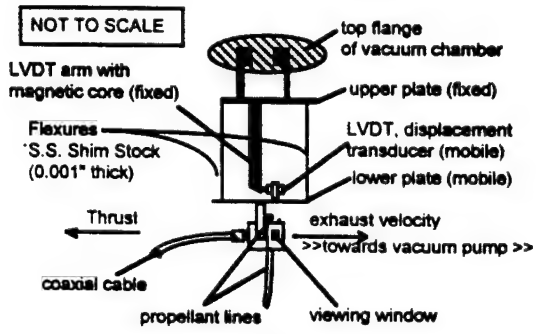

Fig. 6: Pendulum thrust stand

The initial goals of this program are to experimentally obtain values for thrust, specific impulse and thruster efficiency at low microwave power levels. Each of these values are obtained from mass flow and thrust measurements. Equations 2 and 3 show the formulas for computing specific impulse and overall thermodynamic efficiency. Mass flow measurements come from the UNIT mass flow controller with calibration traceable to NIST standards.

$$I_{sp} = \frac{\tau}{mg} \quad (2)$$

$$\eta_{overall} = \frac{\tau^2}{2 \cdot m \cdot P_{input}} \quad (3)$$

Weight is suspended from a thin cotton thread to accurately calibrate the pendulum thrust stand. This calibration is done with at least six different weights ranging from 1.3 to 3.4 grams, which translates to forces ranging from 12.5 to 33.4 mN. The calibration is done prior to each series of tests. Figure 7 shows typical calibration curves prior to cold-gas testing with helium and nitrogen. The two curves represent two different days of testing.

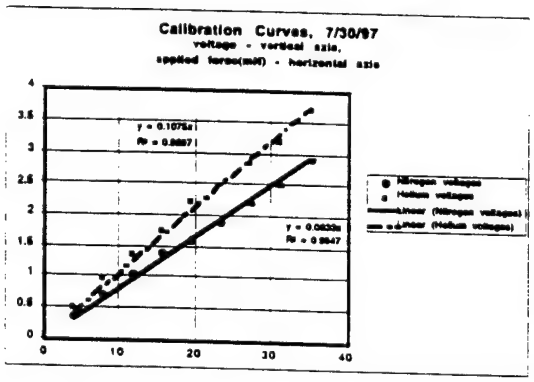

Figure 7: Thrust stand calibration.

Linear regression of the calibration data gives an equation to relate the differential voltage read from the transducer directly to thrust.

Results:

Cold flow data has been obtained for both helium and nitrogen. Tabulated cold flow results are below in Table 1. Ideal Isp values were calculated by CET (1993 version). Helium matches ideal values quite well, while nitrogen is slightly lower than expected. The results of the cold flow testing are very close to expected values. A photo of the thruster installed on the thrust stand for cold-gas testing is shown in Figure 8.

Sustained helium plasma was formed at ambient conditions with a chamber pressure of 5 kPa (gauge) and an incident power level of 20 Watts. The plasma was elliptical and correctly positioned near the nozzle along the cavity's longitudinal axis.

	Nitrogen	Helium
Thrust(mN)	6.568	3.562
mass flow (mg/sec)	17.864	4.428
Isp (sec)	37.48	82.01
Ideal Isp (sec)	42.30	82.40

Table 1: Cold flow results.

Figure 8: Photo of cold-gas testing.

Conclusions:

The microwave arcjet has advantages over conventional arcjets in use today. The electrodeless design eliminates cathode erosion problems associated with DC arcjet types. Due to the tangential swirl injection of the propellant for plasma stabilization, the limited chamber temperature associated with material aspects of resistojets is also increased due to the plasma's axial location and the cold propellant gas's injection from the wall. The 12,000 K plasma formed by the resonant microwave energy should offer high specific impulse at low incident power (~ 100 W). Thrust levels of 30 mN and specific impulse values near 500 seconds are expected for ammonia propellant. The microwave arcjet shows great promise for low thrust applications

such as deep-space missions and geosynchronous North-South station-keeping.

Cold flow testing has been performed in ambient conditions with helium and nitrogen. Helium plasma has been ignited with 20 Watts of microwave power at 5 kPa (gauge) chamber pressure.

Future work for this project includes thrust stand measurements in vacuum. The work will include thrust, specific impulse, and thruster efficiency measurements for ammonia, nitrogen, helium, hydrogen and water vapor propellants exhausting into a vacuum.

References:

1. Sullivan, D. J., Kline J., Philippe, C., M. M. Micci, "Current Status of the Microwave Arcjet Thruster", AIAA-95-3065, 31st AIAA/ASME/SAE/ASEE Joint Propulsion Conference and Exhibit, San Diego, CA, July 10-12, 1995.

2. Sankovic, J. and Hopkins, J., "Miniaturized Arcjet Performance Improvement", AIAA 96-2962, 32nd AIAA/ASME/SAE/ASEE Joint Propulsion Conference, Lake Buena Vista, FL, July 1-3, 1996.

3. Balaam, P. and Micci. M. M., "Investigation of Stabilized Resonant Cavity Microwave Plasmas for Propulsion", AIAA Journal of Propulsion and Power, Vol. 11, No. 5, September-October 1995, p. 1021 - 1027.

4. Mueller, J. and Micci, M. M., "Microwave Waveguide Helium Plasmas for Electrothermal Propulsion", AIAA Journal of Propulsion and Power, Vol. 8, No. 5, September-October 1992, p. 1017 - 1022.

5. Sullivan, D. J., "Development and Performance Characterization of a Microwave Electrothermal Thruster Prototype". Ph.D. Dissertation, Aerospace Engineering Department, Pennsylvania State University, January 1996.

6. Kline, J., "Thrust Measurements of a Microwave Electrothermal Thruster"., Master of Science Thesis, Aerospace Engineering Department, Pennsylvania State University, August 1996.

7. Manzella, D., Oleson, S., Sankovic, J., Haag, T., Semenkin, A. and Kim, V., "Evaluation of Low Power Hall Thruster Propulsion", AIAA 96-2736, 32nd AIAA/ASME/SAE/ASEE Joint Propulsion Conference, Lake Buena Vista, FL, July 1-3, 1996.

8. Khayms, V. and Martinez-Sanchez M., "Design of a Miniaturized Hall Thruster for Microsatellites", AIAA 96-3291, 32nd AIAA/ASME/SAE/ ASEE Joint Propulsion Conference, Lake Buena Vista, FL, July 1-3, 1996.

9. Willmes, G. F. and Burton, R. L., "Performance Measurements and Energy Losses in a 100 Watt Pulsed Arcjet", AIAA 96-2966, 32nd AIAA/ASME/SAE/ASEE Joint Propulsion Conference, Lake Buena Vista, FL, July 1-3, 1996.

10. Weinstein, M. Mictron Inc., Sarasota, FL, *Personal Communication*, 7/7/97

11. Balanis, C. A., "Advanced Engineering Electromagnetics", 1989.

AIAA 99-2717

Low-Power Microwave Arcjet Testing: Plasma and Plume Diagnostics and Performance Evaluation

F. J. Souliez, S. G. Chianese, G. H. Dizac and M. M. Micci

Propulsion Engineering Research Center
Department of Aerospace Engineering
The Pennsylvania State University
University Park, PA 16802

35th AIAA/ASME/SAE/ASEE Joint Propulsion Conference and Exhibit
20–24 June 1999
Los Angeles, California

LOW-POWER MICROWAVE ARCJET TESTING: PLASMA AND PLUME DIAGNOSTICS AND PERFORMANCE EVALUATION

F. J. Souliez*, S. G. Chianese*, G. H. Dizac* and M. M. Micci†
Department of Aerospace Engineering
The Pennsylvania State University
University park, PA 16802

Abstract

The results of an experimental study of a microwave thruster are presented. Performance evaluation of a 7.5 GHz engine was done using different propellants under both atmospheric and vacuum conditions. Helium, nitrogen and ammonia were tested providing mean chamber stagnation temperature values. Other experiments include plasma and plume diagnostics. Emission spectroscopy of the plasma was made in order to measure the plasma electron temperature at different specific power levels, and the commonly-made assumption of Local Thermodynamic Equilibrium (LTE) was examined. In order to obtain thrust and specific impulse data under vacuum conditions, the Doppler shift between light emitted by the exhaust plume parallel to the gas velocity and perpendicular to the flow was measured using a high spectral resolution Fabry-Perot interferometer, yielding centerline specific impulse values for helium propellant at various specific powers. Thrust and mean specific impulses for all three propellants are being measured using a vertical mechanical thrust stand mounted inside a vacuum tank.

Nomenclature

f_r	= resonant frequency
γ	= specific heat ratio
P_o	= mean chamber pressure
T_o	= mean chamber temperature
T_e	= electron temperature
I_{sp}	= specific impulse
P_{cavity}	= power absorbed by cavity
$P_{reflected}$	= power reflected by cavity
$P_{forward}$	= power forwarded to cavity
SP	= specific Power
λ	= emission wavelength
$\Delta\lambda$	= Doppler shift
ν	= emission frequency
c	= speed of light
η	= coupling efficiency

Introduction

Although propulsion systems on the majority of space vehicles to date have consisted of chemical thrusters, an increasing number of spacecraft launched recently use electric propulsion devices. Many of these systems consist of either ion thrusters, which have been under development for almost 35 years[1], or arcjet thrusters manufactured by Primex Aerospace[2] and now offered by Lockheed-Martin, as a high-performance alternative for geosynchronous satellite North-South Station Keeping (NSSK).

The increasing interest in electric propulsion derives from much higher specific impulses relative to chemical thrusters, coupled with technological advances in power subsystem capabilities[3]. However, some of these systems do not fit all types of missions. Ion engines exhibit high efficiencies in Isp's between 3000 and 9000 seconds. These values result in thrust levels that are too low for near-earth missions at typical power levels of 1 to 10 kW. These systems generate very low thrust levels that are inefficient for drag make-up operations or require too much time for orbit insertion maneuvers[4]. The optimal specific impulses for

* Graduate Research Assistant, Student Member, AIAA.
† Professor, Associate Fellow, AIAA.

orbit-raising and in-orbit maneuvering are in the 1000-2000 second range in which ion thrusters are quite inefficient[5].

Conventional arcjets suffer from cathode erosion problems[6] as well as decreased efficiencies when operating in lower power ranges[7]. Operation at 250 W on simulated ammonia yielded specific impulse levels from 360 to 470 seconds, with corresponding efficiencies of between 0.28 and 0.36. Arcjets also cannot operate efficiently in a pulsed mode required for attitude control. Resistojets have a material-based limitation that the propellant gas temperature cannot exceed the maximum allowable temperature of the heating element or any other propellant-wetted surface.

Outside the class of electrothermal thrusters, Hall thrusters operating at 300 W have given specific impulses up to 1160 seconds with hydrazine and a corresponding efficiency of only 0.32[8]. Performance measurements have also been taken with a Hall thruster operating at power levels from 250 W down to 90 W using xenon propellant: the corresponding efficiencies and specific impulses went from 0.31 and 1230 seconds respectively down to 0.14 and 521 seconds respectively[9].

Microwave thrusters are electrothermal thrusters which are electrodeless and therefore do not suffer life limitations of electrode erosion. A systematic illustration is given in Figure 1 showing the major components of a microwave propulsion system.

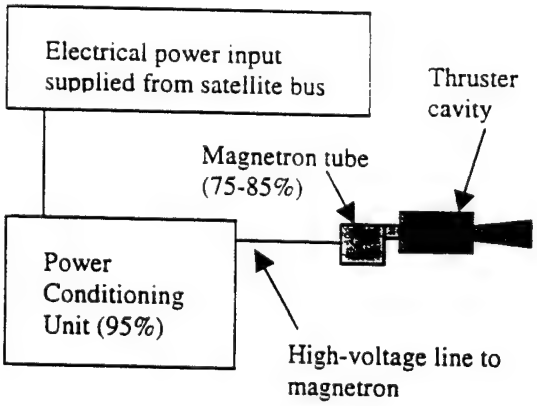

Figure 1 – System illustration with component efficiencies

Microwave resonant cavity thrusters can be distinguished from other electrothermal engines such as arcjets or resistojets by their method of heating the propellant gas. Arcjets use an electric-arc discharge to heat the propellant whereas resistojets use electrical heating through a wall to increase the propellant stagnation temperature. In the case of the microwave thruster, the energy of standing microwaves inside a resonant cavity is absorbed by the incoming propellant without contacting any of the engine's elements.

Previous research on microwave heated propulsion had utilized much higher power levels (up to 2,200 Watts CW) with plasmas confined in one single type of resonant cavity at 2.45 GHz. Over the past three years, the program has shifted from 2-kW-class thrusters to the development of lower power microwave thrusters operating at power levels down to 70 W.

Experiment

The system introduces the microwaves into the engine illustrated in Figure 2. As can be seen, the cavity is partitioned in two halves separated by a dielectric quartz plate. The propellant is swirl-injected tangentially into the nozzle side of the cavity (plasma chamber). This is done for both cooling of the chamber interior walls and for radial stability of the plasma. The other side near the antenna is kept pressurized to ensure that the plasma formation takes place only in the plasma chamber where the propellant is fed in at lower pressure and brought slowly up to the desired chamber pressure.

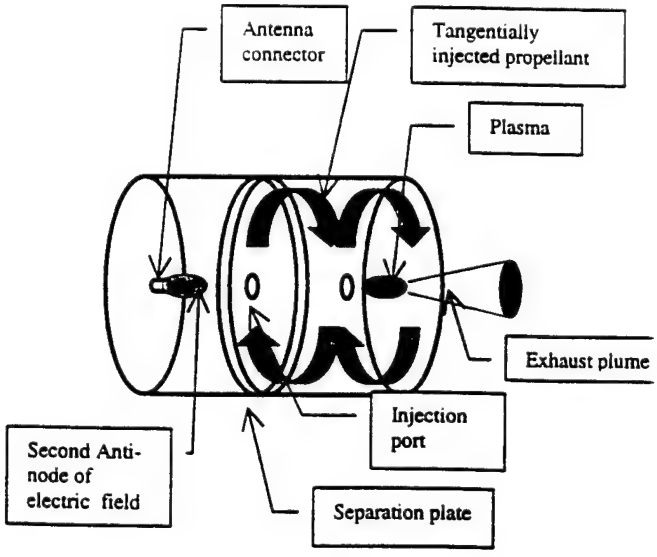

Figure 2 – Schematic of microwave thruster

The plasma is created by the region of high electric field strength formed on the axis of the cavity near the nozzle. The propellant gas is heated by being forced to flow in close contact to the plasma as it expands through the nozzle converting thermal energy to directed kinetic energy, creating thrust.

This design has been tested at two resonant frequencies and proven to be effective with propellants such as gaseous nitrogen, helium, hydrogen, ammonia and water vapor[10]. At low power levels (<70 Watts), vacuum starts have been successful with both types of engines (2.45 GHz engine and 7.5 GHz engine) using helium, nitrogen or ammonia as propellant. A vacuum start is a procedure that brings the resonant cavity to a pressure low enough for the microwave breakdown to occur and the plasma to form, thus simulating realistic start-up conditions in space. Coupling efficiencies between the injected gas and the incoming microwave energy up to 99% have been measured.

Propellant Testing

The goals of this experiment were to obtain values for plasma chamber stagnation pressure, specific powers and cavity efficiencies. Each of these values could be obtained from pressure, power and mass flow rate measurements. Equations 1, 2 and 3 give the formulas for specific power and cavity coupling efficiency.

$$P_{cavity} = P_{forward} - P_{reflected} \qquad (1)$$

$$SP = \frac{P_{cavity}}{\dot{m}} \qquad (2)$$

$$\eta = \frac{P_{cavity}}{P_{forward}} \qquad (3)$$

The other objective was to test the 7.5 GHz thruster in vacuum conditions in order to characterize the operation of the thruster with respect to its start-up behavior and achievement of steady-state operation at low power levels using various propellant gases (helium, nitrogen and ammonia). During these tests, the vacuum tank was pumped using only a Stokes mechanical pump. The experimental setup is illustrated in Figure 3.

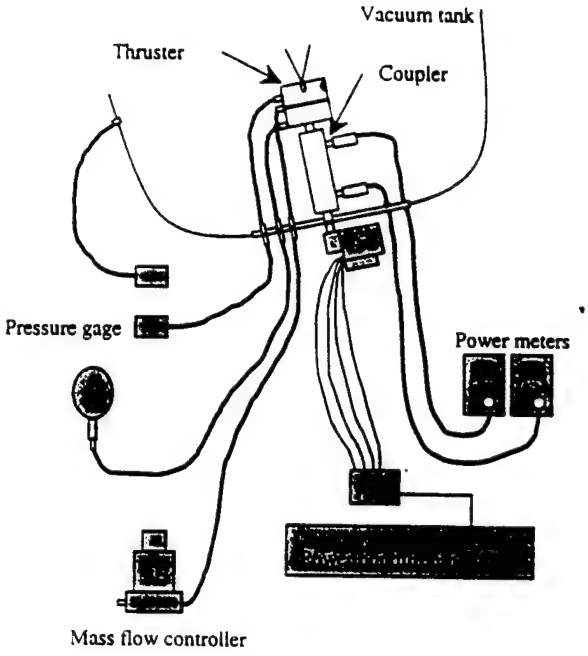

Figure 3 – Schematic of assembly used during vacuum tank testing

This testing showed that the low-power thruster could be operated autonomously under realistic conditions and for extended periods without any damage to any component. Most of the testing has concentrated on the 7.5 GHz cavity using all three propellants since no significant thruster chamber pressure level could be reached using the 2.45 GHz engine before the plasma would extinguish.

Tables 1, 2 and 3 present data that were collected using all three propellants including mass flow rate, microwave power input to plasma, chamber stagnation pressure, coupling efficiency, η, between input microwave power and plasma, and specific power from initial start-up to steady-state conditions.

The data show that the plasma chamber pressure could be brought up to 45 psia with a stable helium plasma in place absorbing a power slightly less than 70 W. A higher pressure of 54 psia could be achieved by increasing the power inside the cavity up to 77 W with a corresponding coupling efficiency of 98.5% or more. Stable nitrogen plasmas could be maintained at pressure levels up to 55 psia with coupling efficiencies between the gas and the incoming microwave power above 98%. The orientation of the thruster within the vacuum tank combined with buoyancy forces resulted in nitrogen plasmas being generally less stable than helium plasmas. Data with ammonia plasmas

could be recorded with chamber pressures up to 7 psia with coupling efficiencies above 86%.

$\dot{m}$ (mg/sec)	P_{cavity} (W)	P_0 (psia)	η (%)	SP (MJ/Kg)
2.16	34.5	8.85	55.0	15.97
4.32	47.9	21	64.3	11.08
6.48	65.6	30.25	98.5	10.12
12.37	67.1	45.28	98.5	5.42
14.41	77.0	54.00	98.7	5.34

Table 1 – Helium hot-firing data in vacuum

$\dot{m}$ (mg/sec)	P_{cavity} (W)	P_o (psia)	η (%)	SP (MJ/Kg)
2.60	76.4	4.71	76.5	29.38
7.81	67.9	11.0	98.5	8.69
10.42	67.9	24.6	98.5	6.52
14.59	67.9	32.7	98.5	4.65
20.32	86.0	50.0	99.0	3.66
26.05	86.0	55.0	99.0	3.30

Table 2 – Nitrogen hot-firing data in vacuum

$\dot{m}$ (mg/sec)	P_{cavity} (W)	P_o (psia)	η (%)	SP (MJ/Kg)
0.65	72.5	4.18	98.6	113.54
0.83	65.4	4.86	98.2	78.79
0.97	58.5	5.45	94.4	60.31
1.07	57.3	5.95	89.1	53.55
1.28	86.0	7.13	86.0	67.19

Table 3 – Ammonia hot-firing data in vacuum

The different plasma pressure levels that could be attained are of the same order of magnitude as those encountered during previous investigations at much higher power levels[11,12]. The difference in behavior between helium plasmas and other molecular propellants, in that for a given microwave power a helium plasma can be sustained at higher pressures, had also been observed at higher power levels[13]. The most probable explanation is that helium is monatomic whereas the other propellants are diatomic or polyatomic molecules. The helium atom has few modes of internal energy storage; because of this, inelastic collisions with high energy electrons are highly effective in liberating free electrons and creating helium ions. On the other hand, the polyatomic propellants have a relatively large number of internal modes of energy storage when compared with the helium atom. Inelastic collisions that would ionize a helium atom may act only to simply excite an internal mode of the polyatomic molecule.

Another argument to explain the premature loss of molecular plasmas is the difference in thermal conductivities of helium and other polyatomic propellants at high temperatures; 0.25 W/(m°K) for helium, 0.067 W/(m°K) for ammonia gas and 0.044 W/(m°K) for nitrogen[14]. The reduced values of the thermal conductivities of nitrogen and ammonia result in a decrease in the effective volumetric area the thermal energy of the plasma core can influence, thus limiting the amount of heat transferred from the plasma to the swirling cold propellant gas. Such a limitation on the maximum attainable enthalpy rise restrains the thruster chamber pressure from reaching pressure levels of the order of magnitude of that of helium propellant when using the same amount of microwave power.

A reliable manner to determine the temperature rise once the plasma forms inside the cavity is to compare the pressure values for a given mass flow rate between cold flows and hot-firings. As shown in Equation 4, forming their ratio allows us to eliminate the throat area A which is known with a very poor precision due its small size, 0.25 mm ID. The procedure requires several iterations: an initial inlet temperature has to be assumed in order to have the corresponding γ-value, then the chamber stagnation temperature can be evaluated using Equation 4 and compared with the initial guess. This is done until both values coincide. This gives a set of mean chamber stagnation temperature values that are plotted in Figures 4(a) to 4(c) for helium, nitrogen and ammonia propellants respectively.

As expected, the inlet temperature for ammonia propellant is relatively low, since some of the microwave energy absorbed by the ammonia gas goes into various energy storage modes such as vibrational or rotational modes instead of raising the translational energy of the

$$\frac{T_{0hot}}{T_{0cold}} = \left(\frac{P_{0hot}\sqrt{\gamma_{hot}}\left(\frac{2}{\gamma+1}\right)^{\frac{\gamma+1}{2(\gamma-1)}_{hot}}}{P_{0cold}\sqrt{\gamma_{cold}}\left(\frac{2}{\gamma+1}\right)^{\frac{\gamma+1}{2(\gamma-1)}_{cold}}} \right)^2 \quad (4)$$

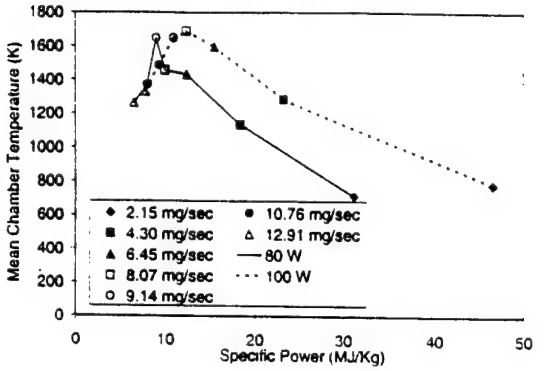

(a)

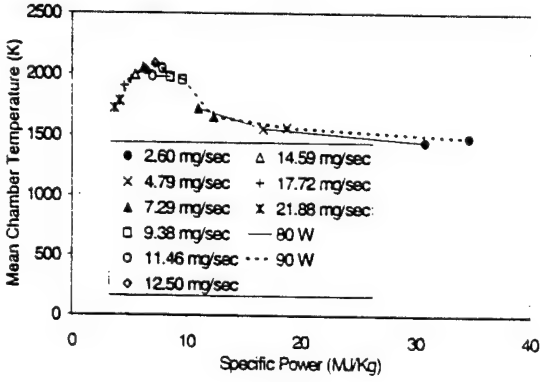

(b)

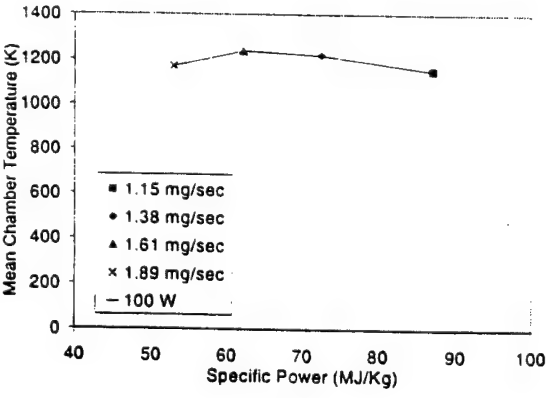

(c)

Figure 4 – Measured mean chamber stagnation temperature for (a) helium, (b) nitrogen and (c) ammonia propellants at various power levels.

propellant, i.e. its temperature. The variations of temperature are dominated by the location of the plasma. At high mass flow rates, the resonance frequency is such that the plasma is right next to the nozzle inlet, whereas at low flow rates, it tends to stay away from the nozzle. This determines how heat is transferred to the cold propellant gas before exiting the chamber.

Testing so far of the larger cavity 2.45 GHz thruster has produced stable plasma discharges using helium, nitrogen and ammonia. Plasma chamber pressure levels up to 16 psia have been obtained using helium propellant. The 2.45 GHz thruster chamber pressure has been brought up to 5 psia using nitrogen or ammonia.

Electron Temperature Experiment

Emission spectroscopy provides a non-intrusive method of determining the temperature of gaseous discharges. It does not require the use of probes exposed to the plasma that might change its properties. The present work focused on the measurement of the free electron temperature T_e. In order to determine that quantity accurately, possible deviations from thermal equilibrium behavior within the plasma had to be evaluated as well as their impact on the selected spectroscopic method.

Most of the data were taken well above atmospheric pressure levels. Previous investigations in argon plasmas by Eddy[15] indicate that the heavy particle temperature approaches the electron temperature at this level of pressure. Many techniques have been considered, essentially absolute continuum spectroscopy and relative line intensity, the latter being the one chosen for use. In all cases, because of the Local Thermodynamic Equilibrium (L.T.E.) assumption involved, the obtained temperature values must be interpreted very carefully. This method is the most commonly used spectroscopic diagnostic to determine the electron temperature inside laboratory plasmas. It consists in determining the relative intensities of two spectral lines. It may be shown that for two emission lines at the wavelengths λ_A and λ_B,

$$\frac{I_A}{I_B} = \frac{(\nu g_2 A_{21})_A}{(\nu g_2 A_{21})_B} e^{-(E_{2A}-E_{2B})/kT_e} \quad (5)$$

where I_A and I_B are the intensities measured at the wavelengths λ_A and λ_B respectively. The frequency ν, the transition probability A, the degeneracy g, and the upper energy level E are known constants. The electron temperature T_e

can then be evaluated from the following expression.

$$T_e = \frac{1}{k} \frac{E_{2_B} - E_{2_A}}{\ln\left(\frac{I_A (\upsilon g_2 A_{21})_B}{I_B (\upsilon g_2 A_{21})_A}\right)} \qquad (6)$$

where the energy gap E_{2A}-E_{2B} has to be as large as possible for this method to be temperature sensitive[16]. Another condition is that the plasma pressure must be as high as possible to minimize deviation from L.T.E. assumptions, as described in the following equation:

$$\frac{\Delta T}{T_e} = \frac{T_e - T_g}{T_e} = \frac{(\lambda_e E)^2}{\left(\frac{3}{2} k T_e\right)^2} \frac{M}{8 m_e} \qquad (7)$$

The temperature difference T_e-T_g between electrons and heavy particles, and thus the degree of non-equilibrium can only be decreased at high pressures (small mean free path length λ_e) and low power levels (small electric field strength E). Another issue is that the transitions must correspond to the highest states that can be detected by the optical setup for the L.T.E. assumptions to be valid. High-collision rates are the predominant factor that can bring the plasma to equilibrium. Large upper quantum state numbers, n, correspond to larger collision cross-sections σ (e.g. σ is proportional to n^4 for excited hydrogen atoms). As shown in the equation below, the time t between two consecutive collisions is short when the collision cross section is large, and hence departures from L.T.E. are small[17].

$$t = \frac{1}{N_e \sigma V} \qquad (8)$$

The spectroscopic measurement is performed by collecting the light emitted by the plasma through the engine viewing window. The spectroscopic system that is used throughout the different experiments is shown in Figure 5.

The collected light is focused on the entrance slit of the spectrometer which is a 0.5 m, f/6.9 Czerney-Turner system. A 1,200 lines/mm Bausch & Lomb ruled grating is used. This spectrometer / grating combination imposes an upper limit to the wavelengths which may be detected of 660 nm. Connected to the output of

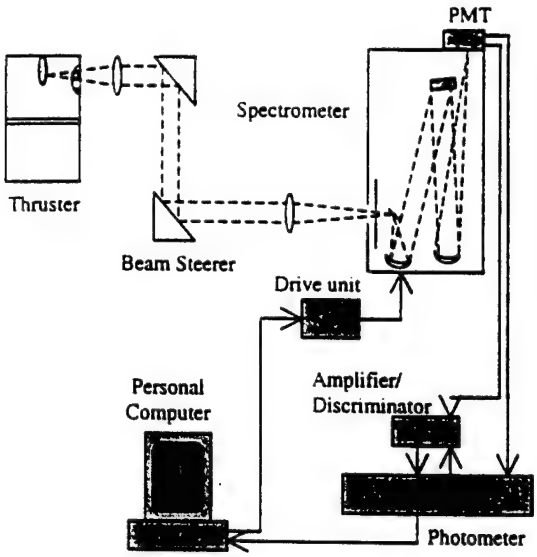

Figure 5 – Schematic of optical setup used in the electron temperature experiment

the spectrometer is a Hamamatsu 1P28A photomultiplier tube (PMT) with a detection range from 185 nm to 700 nm and a maximal spectral response at 450 nm. The quantum efficiency of the PMT over the visible range had to be calibrated by its manufacturer, as well as the diffraction grating efficiency of the spectrometer. This is meant to obtain the true intensity values from the measured intensities correcting for the various instrumental sensitivities. The PMT serves to amplify the signal which is then further amplified and converted into an electric current analog signal by a Pacific Instruments Model 126 photometer. The spectrometer control and data acquisition was performed by a personal computer with a Data Translation series A/D board driven by a BASIC program.

A set of four lines of helium λ = 5876Å (upper quantum level n = 3), λ = 5016Å (n = 3), λ = 4922Å (n = 4) and λ = 4471Å (n = 4) was scanned twice for each set of operating conditions. This was meant to check for the repeatability of the measurements in time. The lines corresponding to higher quantum numbers were either out of range of the spectrometer or of too low intensity to be detected by the instruments.

For the reasons mentioned above, the data were collected at increasing pressure levels and the commonly made assumption of Local Thermodynamic Equilibrium (L.T.E.) has been examined. The lowest operating plasma chamber

pressure was 28 psia: this corresponds to twice the minimum pressure value for which the L.T.E. assumption is usually made i.e. one atmosphere. The highest testing pressure was 50 psia: this is mainly due to the injection pressure limitation across the digital mass flow controller that cannot exceed 50 psia, as well as the design of the engine, since the pressure differential across the separation plate cannot exceed 50 psia.

In these conditions, the resultant line broadening mechanism is dominated by the pressure broadening effect (or Stark effect), so that the line intensities were corrected assuming a Lorentzian shape profile out into the far wings. Huddlestone[18] gave the two following equations to evaluate the whole energy associated with each peak,

$$\frac{\Delta\lambda^{*}_{B}}{\Delta\lambda^{t}_{1/2}} = \left[\left(\frac{\Delta\lambda^{*}_{B}}{\Delta\lambda^{*}_{1/2}}\right)^{2} - 2\right]^{1/2} \qquad (9)$$

$$\frac{I^{t}}{I^{*}} = \frac{\pi}{2}\left[\tan^{-1}\left(\frac{\Delta\lambda^{*}_{B}}{\Delta\lambda^{t}_{1/2}}\right) - \left(\frac{\Delta\lambda^{*}_{B}}{\Delta\lambda^{t}_{1/2}} + \frac{\Delta\lambda^{t}_{1/2}}{\Delta\lambda^{*}_{B}}\right)\right] \qquad (10)$$

where I^{t} is the true line intensity and $\Delta\lambda^{t}_{1/2}$ the true half-width at full maximum, both recovered from the measured values I^{*}, $\Delta\lambda^{t}_{1/2}$ and $\Delta\lambda^{*}_{B}$ (half-width of the truncated base of the peak). Only the data satisfying a 15% repeatability between each scan were used to estimate the electron temperature.

Using Equation 6 combined with the reading of different scans, some valuable electron temperature values could be determined for various pressure conditions. The frequency ν, the transition probability A, the degeneracy g, and the upper energy level E needed to evaluate T_e were from 5% to 15% accurate[19]. The different temperature values for each emission line and each set of operating conditions are listed in Table 4.

These values are much lower than those obtained by Mueller and Micci[20] or Balaam and Micci[21,22] during previous spectroscopic investigations. This can be explained by several factors: their data were collected at much higher power levels, and as mentioned before, the absolute continuum technique was used. Generally, the electron temperature values obtained with their method ranged from 11,000 °K up to 12,500 °K.

These values show that at 28 psia, the plasma is far from L.T.E. conditions, otherwise each line ratio would yield the same value. As expected, the temperature values tend to converge towards one single value around 4,000 °K as the plasma pressure increases to 50 psia. The dispersion of the average values goes from 75% down to 18%. The measured temperatures for the line ratios at 50 psia can be assumed to be very close considering that the calculation of the temperature is subject to both experimental errors and errors arising from uncertainties in the spectroscopic constants that are employed. The

P_0 (psia)	$T\left(\frac{I_{\lambda=5876}}{I_{\lambda=4922}}\right)$ (°K)	$T\left(\frac{I_{\lambda=5876}}{I_{\lambda=4771}}\right)$ (°K)	$T\left(\frac{I_{\lambda=5016}}{I_{\lambda=4922}}\right)$ (°K)	$T\left(\frac{I_{\lambda=5016}}{I_{\lambda=4471}}\right)$ (°K)	$\frac{\sum T}{4}$
28	10078	5893	3946	3077	5749 ±75 %
37	5892	5635	3166	2982	4419 ±33 %
50	4865	4147	3726	3283	4005 ±18 %

Table 4 – Electron temperature data

relative error in the temperature is related to any error through Equations 11 and 12.

$$\left|\frac{\Delta T}{T}\right| = \frac{kT}{E_2 - E_1}\left|\frac{\Delta X}{X}\right| \qquad (11)$$

$$X = \frac{(\upsilon g A)_2 I_1}{(\upsilon g A)_1 I_2} \qquad (12)$$

where experimental errors in $\Delta X/X$ are rarely below 0.1, and the prefactor of this quantity is typically of order 1. This suggests a ±10% error in electron temperatures from such line ratios, even under favorable conditions concerning the validity of L.T.E. conditions and the availability of accurate A-values. Those results were encouraging enough so that no attempt was made to use the absolute continuum technique.

Doppler Shift Experiment

If light is emitted from a particle moving toward a detector, the frequency of that light will be shifted. If this shift can be measured, then the velocity u at which the molecule was moving toward the detector can be calculated as,

$$u = \frac{c\Delta\upsilon}{\upsilon} \qquad (13)$$

where ν is the frequency of a reference signal, c the speed of light and $\Delta\nu$ the Doppler shift between the moving particle and the reference signal. This application assumes that the gas exiting the nozzle is either self-radiant (i.e. a high temperature plasma exhaust) or can be induced to fluoresce using some type of excitation process (i.e. laser induced fluorescence). This technique as applied to electrothermal thrusters has primarily concentrated on resolving the velocity profile of the atomic hydrogen species within the exhaust plume. In our case, this has mainly been used to characterize the exhaust plume of helium plasmas. A picture of a helium plasma plume is shown in Figure 6. The nozzle area ratio is 52:1.

In practice, the lens that is supposed to collect the Doppler-shifted signal is slightly off-axis so that the unshifted pressure-broadened signal from the plasma inside the cavity does not override through the nozzle the shifted emission

Figure 6 - 7.5 GHz thruster helium firing in vacuum

from the plume. A picture of the collection optics is shown in Figure 7.

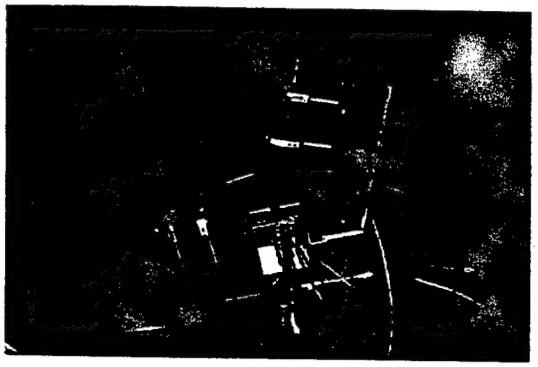

Figure 7 – Picture of the optical assembly mounted inside the vacuum vacility

The instruments needed for this experiment are very similar to those required for the electron temperature measurement. Some critical elements had to be added in order to be able to measure the Doppler shift, including a high spectral resolution Burleigh TL-15 Fabry-Perot interferometer and two high-transmittance fiber optical cables mounted with special collimators.

Centerline specific impulses have been measured for specific powers ranging from 15 up to 30 MJ/Kg using helium propellant with an input power of 80 W. The Doppler-shift was evaluated using the emission line corresponding to a wavelength of 5876 Å. At lower specific power levels (corresponding to higher mass flow rates), the lines were pressure-broadened so that the shift could not be resolved for pressures above 31 psia. Figure 8 clearly shows that the

centerline shift can be accurately measured at high specific power values.

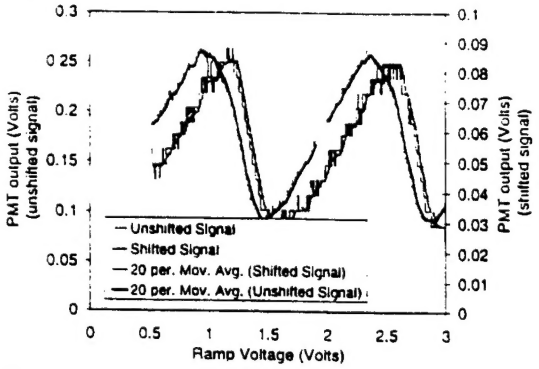

Figure 8 – Trace of Fabry-Perot etalon output at high specific power

For verification purposes, several scans of the plume seen from the same angle in the same operating conditions were compared to check that no significant drift occurs. Figure 9 is a summary of all the data points collected between 15 and 30 MJ/Kg.

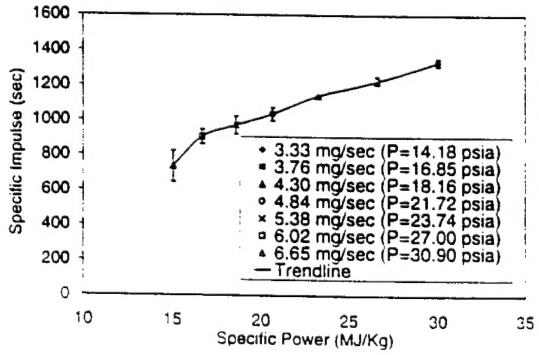

Figure 9 – Specific impulse vs. specific power for helium propellant at 80 W

As expected these plots show that specific impulse increases with specific power. The error bar is bigger for low specific power results since the plume was pressure-broadened and the expected specific impulse was lower, thus making the discrimination between two closely spaced lines more difficult. No result could be obtained at higher specific power levels, mainly due to the low light intensity of the plume at low pressure, thus limiting the maximum specific impulse that could be experimentally measured.

Thrust Measurement

Thrust measurements are required in order to determine the performance of the microwave arcjet. Previously, Nordling[23] employed an inverted pendulum stand for use with the thruster operating in a horizontal configuration. Thrust measurements were taken in ambient conditions. However, buoyancy effects caused plasma instability and a loss of measured thrust. In order to eliminate these losses, a stand that allows the thruster to operate in the vertical position was developed.

A resolution of 1 mN or better is desired. To achieve this, the 5 kg mass of the thruster system must be counterbalanced. This is done with a lead counterweight attached to a knife-edge fulcrum system. Figure 10 shows a schematic of the system.

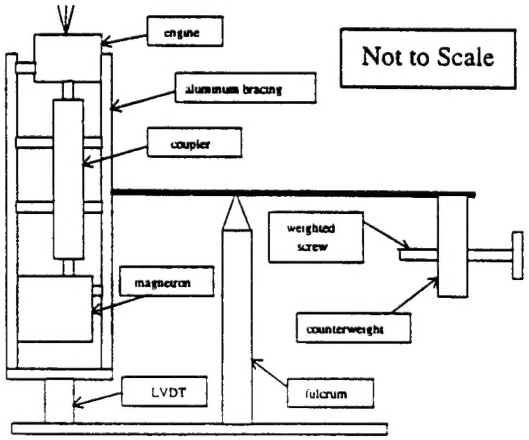

Figure 10 -Test Stand Schematic

The thruster system has a moment arm of 10 cm, and the counterweight has a moment arm of 28.5 cm. The lever arm is attached to the thruster system and counterweight above their respective centers of mass, to provide inherent rotational stability. To finely balance the system, a fully threaded six inch screw can be adjusted. When the engine is fired, the thruster system displaces downward. For small angular rotations the motion is proportional to the applied thrust. A force sensing Linear Variable Differential Transducer (LVDT) is used to measure the thrust.

For analysis, the fulcrum is assumed to be frictionless. The largest thrust expected,

approximately 50 mN, causes a vertical deflection of no more than 0.05 mm. The resulting angular deflection is no more than 0.035 degrees. This allows the restoring force of gravity to be neglected. The sensitivity of the system is dominated by the limitations in the electronics. The LVDT, and thus the test stand, has a resolution of approximately 0.5 mN, which is within the desired range.

The test stand is used while the thruster is operating in the vacuum tank. During firings the vacuum pump is not operational because the vibrations cause too much noise in the system. Because the power not absorbed by the propellant is reflected back to the magnetron, the microwave generating device must be cooled. This is done by flowing two jets of helium gas against the sides of the magnetron after each test. The vacuum tank is evacuated during and after this process. The stand is calibrated by placing known masses on the thruster and recording the response before the vacuum pump is operated for the first time each testing session.

The test stand will be used to determine the thrust and specific impulse produced by the microwave arcjet with helium, nitrogen, and ammonia as propellants for several power levels and mass flow rates.

Conclusion

The ability to create and maintain plasmas at low microwave power levels under realistic space conditions has been demonstrated with propellants such as helium, nitrogen and ammonia. Mean chamber stagnation temperatures could be measured, employing an iterative process providing inlet temperatures as high as 1700 °K for helium propellant, 2100°K for nitrogen propellant and 1240°K for ammonia propellant. As expected, a large fraction of microwave power is lost in various energy storage modes of ammonia molecules, hence reducing its enthalpy rise.

Spectroscopic measurements using the relative line intensity method have yielded electron temperature values for helium converging to an average value of 4000 °K with less than 100 W of input power. The LTE assumption has been validated at pressure levels approaching 50 psia.

The Doppler shift experiment has been successful and has produced centerline specific impulse values ranging from 730 seconds up to 1330 seconds for specific powers between 15 and 30 MJ/Kg with helium propellant. It has not been possible yet to produce data using ammonia propellant due to strong background emissions.

Acknowledgements

This work was supported by AFSOR Grant F49620-97-1-0117.

References

[1]Schreib, R., "Utility of Xenon Ion Statiokeeping", AIAA Paper 86-1849, June 1986.

[2]Smith, R. D., Yano, S. E., Armbruster, K., Roberts, C. R., Lichtin, D. A., and Beck, J. W., "Flight Qualification of a 1.8 kW Hydrazine Arcjet System," IEPC Paper 93-007, 23rd International Electric Propulsion Conference, Sept 1993.

[3]Bennett, G. L., Brandhorst, Jr., Bankston, C. P., and Sovie, R. J., "An overview of Electric Power: A Key Technology for Electric Propulsion", IEPC 97-006, 25th International Electric Propulsion Conference, August 24-28, 1997.

[4]Keiser, T. L., and Micci, M. M., "Application of Microwave Thrusters for Stationkeeping and Orbit Raising on the INTELSAT Series Communication Satellites", IAF 90-228, 41st Congress of the International Astronautical Federation", October 6-12, 1990.

[5]Hill, P. G., and Peterson, C. R., Mechanics and Thermodynamics of Propulsion, Addison-Wesley, 1965, Reading, MA.

[6]Nordling, D. and Micci, M. M., "Low Power Microwave Arcjet Development", IEPC 97-089, 25th International Electric Propulsion Conference, August 24-28, 1997.

[7]Sankovic, J. and Hopkins, J., "Miniaturized Arcjet Performance Improvement", AIAA 96-2962, 32nd AIAA/ASME/SAE/ASEE Joint Propulsion Conference, Lake Buena Vista, FL, July 1-3, 1996.

[8]Manzella, D., Oleson, S., Sankovic, J., Haag, T., Semenkin and A., Kim, V., "Evaluation of Low Power Hall Thruster Propulsion", AIAA 96-

2736, 32nd AIAA/ASME/SAE/ASEE Joint Propulsion Conference, Lake Buena Vista, FL, July 1-3, 1996.

[9]Jacobson, D., and Jankovsky, R., "Test Results of a 200 W Class Hall Effect Thruster", AIAA 98-3792, 34th AIAA/ASME/SAE/ASEE Joint Propulsion Conference, Cleveland, OH, July 13-15, 1998.

[10]Sullivan, D. J., Development and Performance Characterization of a Microwave Electrothermal Thruster Prototype, Ph.D. Dissertation, Aerospace Engineering Department, Pennsylvania State University, January 1996.

[11]Sullivan, D. J., Kline, J., Philippe, C., Micci, M. M., "Current Status of the Microwave Arcjet Thruster", AIAA 95-3065, 31st AIAA/ASME/SAE/ASEE Joint Propulsion Conference and Exhibit, San Diego, CA, July 10-12, 1995.

[12]Balaam, P., Maul, W., and Micci, M. M., "Characterization of Free-Floating Nitrogen and Helium Plasmas Generated in a Microwave Resonant Cavity", IEPC 88-099, 20th DGLR/AIAA/JSASS International Electric Propulsion Conference, Garmisch-Partenkirchen, W. Germany, October 3-6, 1988.

[13]Sullivan, D. J. and Micci, M. M., "The effects of Molecular Propellants on the Performance of a Resonant Cavity Electrothermal Thruster", IEPC 91-034, 22nd AIDAA/AIAA/DGLR/JSASS International Electric Propulsion Conference, Viareggio, Italy, October 14-17, 1991.

[14]Lide, D. R., Handbook of Chemistry and Physics, 74th edition, 1993-1994.

[15]Eddy, T. L., "Low Pressure Plasma Diagnostic Methods", AIAA 89-2830, 25th Joint Propulsion Conference, Monterey, CA, July 1989.

[16]Griem, Principles of Plasma Spectroscopy, Cambridge University Press, 1997.

[17]Dalgarno, A. and Layzer, D., Spectroscopy of Astrophysical Plasmas, New York, Cambridge University Press, 1987.

[18]Huddlestone, R. H. and Leonard, S. L., Plasma Diagnostic Techniques, Academic Press, New York, 1965.

[19]Wiese, W. L., Smith, M. W., and Glennon, B. M., Atomic Transition Probabilities (A Critical Data Compilation), Volume I, Elements Hydrogen Through Neon, Washington, U. S. Dept. of Commerce, National Bureau of Standards, 1966.

[20]Mueller, J., and Micci, M. M., "Microwave Waveguide Helium Plasmas for Electrothermal Propulsion", Journal of Propulsion and Power, Vol. 8, No. 5, Sept.-Oct. 1992.

[21]Balaam, P. and Micci, M. M., "Investigation of Free-Floating Resonant Cavity Microwave Plasmas for Propulsion", Journal of Propulsion and Power, Vol. 8, No. 1, Jan.-Feb. 1992.

[22]Balaam, P. and Micci, M. M., "Investigation of Stabilized Resonant Cavity Microwave Plasmas for Propulsion", Journal of Propulsion and Power, Vol. 11, No. 5, Sept.-Oct. 1995.

[23]Nordling, David A., "High-Frequency Low-Power Microwave Arcjet Thruster Development." Master of Science Thesis, Aerospace Engineering Department, Pennsylvania State University, August 1998.